Master Thesis

Comparative study of reactive oxygen species in mesenchymal stem and osteoblast-like MG-63 cells

carried out for the purpose of obtaining the degree of Master of Science (MSc or Dipl.-Ing. or DI), submitted at TU Wien, Faculty of Technical Chemistry, by

Sergejs Zavadskis

Mat.Nr.:01246578

under the supervision of

Univ.Doz. Univ.Prof. Dipl.-Ing. Dr.techn. Heinz Redl

Institut für Verfahrenstechnik, Umwelttechnik und technische Biowissenschaften

and

Univ.Doz. Dr. Andrey Kozlov

Ludwig Boltzmann Institut für Experimentelle und Klinische Traumatologie

I confirm, that going to press of this thesis needs the confirmation of the examination committee.

Affidavit

I declare in lieu of oath, that I wrote this thesis and performed the associated research myself, using only literature cited in this volume. If text passages from sources are used literally, they are marked as such.
I confirm that this work is original and has not been submitted elsewhere for any examination, nor it is currently under consideration for a thesis elsewhere.

Date: _____

Signature

ACKNOWLEDGEMENTS

Firstly, I would like to thank my family for providing support and encouragement all along the way. Without you, it would not have been possible for me to accomplish this.

I owe a great debt of gratitude to my supervisors, especially Dr. Kozlov for providing guidance, feedback and scientific insight for this project. I would like to thank my lab colleague Sergiu for invaluable assistance in experiment planning and methodology together with the rest of the team for providing supportive and friendly atmosphere.

ABSTRACT

Reactive oxygen species (ROS) are biological molecules known for their high chemical reactivity caused by an unpaired electron on the outer shell of the oxygen atom. For a long time ROS were considered as a toxic byproduct of the cellular metabolism. However, in the last decade, the view on ROS had shifted from being a deleterious metabolic side product to an important molecule playing a significant role in numerous regulatory cell processes. At low physiological concentrations, ROS are engaged in proliferative and regenerative cellular pathways and cellular homeostasis, however, their overproduction is known to cause oxidative stress associated with various diseases. Therefore, a better understanding of ROS metabolism can be implicated in the development of novel drugs and therapies, particularly for tissue regeneration.

The aim of this study was to investigate metabolic pathways of ROS in non-differentiated (human amniotic mesenchymal stromal cells (hAMSC) and differentiated (MG-63 osteoblast-like) cells with emphasis on NOX(NADPH-Oxidase) and mitochondria-derived ROS and possible therapeutic potential of the NOX inhibitor diphenyliodonium (DPI).

By utilizing laser scanning confocal microscopy with ROS-sensitive fluorescent probes in conjunction with specific chemical treatments targeting well defined segments of ROS metabolism, we examined the turnover of cellular ROS in both cell types. In hAMSC, DPI decreased the levels of cytoplasmic ROS. Different concentrations of DPI manifested similar effects in this type of cells. MitoTEMPO, a specific inhibitor of mitochondrial ROS (mtROS), decreased ROS levels in cytoplasm suggesting occurrence of a crosstalk between NOX and mitochondria mediated by ROS. In contrast to hAMSC, MG-63 did not show any decrease in ROS levels in response to low concentration of DPI, but high concentration of DPI acutely increased the concentration of cytoplasmic ROS. The increased levels of ROS were accompanied by a drop in mitochondrial membrane potential, suggesting mitochondria as a predominant ROS source in MG63. The latter was supported by the fact that the release of ROS into the cytoplasm was prevented by mitoTEMPO. The determination of nitric oxide in cytoplasm of MG-63 indirectly suggested the involvement of ONOO- in the damage of mitochondria.

Our data suggest that metabolism of ROS is different in non-differentiated and differentiated cells. In non-differentiated cells, NOX and the crosstalk between NOX and mitochondria predominantly define ROS metabolism, while in differentiated cells ROS is regulated predominantly by mitochondria. DPI potentially can be used to modulate activity of human amniotic mesenchymal stromal cells. Modulation of cellular activity can increase the applicability of hAMSC in tissue regeneration.

LIST OF FIGURES

TABLE OF CONTENTS

CHAPTER I: INTRODUCTION

Background

Reactive oxygen species (ROS) are highly reactive biological molecules with an unpaired electron on the out shell of the oxygen atom. For decades ROS and their sister group of reactive nitrogen species (RNS) have been considered toxic metabolic side products, which activated oxidative stress and were associated with development of numerous pathologies.

ROS were seen as a price for extremely efficient (compared to glycolysis) synthesis of ATP via oxidative phosphorylation in mitochondria, one of the major ROS sources in cells. Billions of years ago specialized bacteria were incorporated in simple prokaryotic cells on the symbiotic base to evolve later in the mitochondria [1]. The distinct properties of this peculiar transition are still present to this day, as mitochondria are the only organelles have their own DNA with own translation and transcription mechanisms as well as enzymatic machinery.

However, what seemed to be deleterious waste product at first glance, turned out to be a part of an intricate system with a multitude of roles. ROS and RNS play an important role in cell signaling processes, and also contribute to the immune response as one of the tools to deactivate bacteria.

ROS are directly involved in a variety of metabolic pathways, and mitochondria turned out to be not the only source of ROS within the cells. A whole group of NADPH-Oxidases (NOX) and nitric oxide synthase (NOS) specialize on ROS production for different purposes.

In this project human mesenchymal stem cells (hAMSC) were chosen as one of the study objects, and MG-63 osteoblast-like cells as the other. Alternative definition of hAMSC as human mesenchymal stromal cells also exists, but in this work we will refer to hAMSC as human mesenchymal stem cells.

Generally, mesenchymal stem cells can differentiate to adipocytes, chondrocytes and osteoblasts [2]. In this project, MG-63 osteoblast-like cell line was chosen as cells representing osteoblasts differentiated from hAMSC. However, this model has certain limitations because this cell line is derived from osteosarcoma, and thus may exhibit cancer-related properties. They represent a model of immature osteoblasts, and therefore mineralisation process is inconsistent. This puts a strong limitation on its application as tissue culture plastic and implant material. However, the response to hormonal treatments was reported to be similar to normal human osteoblast cells compared to other osteoblast cell lines [3], suggesting that MG-63 cells are a suitable model for metabolic research, such as ROS metabolism.

hAMSC are very promising stem cell type for due to their multipotency and very little ethical concern related to their origin and harvest, as they can be extracted from childbirth waste material.

They have been already proven to be capable of playing a vital role in novel stem cell-related therapies, and in this project we are trying to look at how manipulating ROS can affect hAMSC metabolism.

Reactive oxygen and nitrogen species

Two classes molecule classes consisting of reactive oxygen species (ROS) and reactive nitrogen species (RNS) comprise together a family referred as RONS, characterized by unpaired electrons on the outer shell of oxygen or nitrogen atoms.

The ROS include superoxide (O_2^-), hydrogen peroxide (H_2O_2) and hydroxyl radical ($\cdot OH$). The superoxide primarily originates as a side product of oxidative phosphorylation in the mitochondria, and from certain types of NADPH oxidase (e.g. NOX2).

Hydrogen peroxide originates as a product of superoxide; this reaction is catalyzed by superoxide dismutase (SOD). NADPH Oxidase 4 also has been identied as an enzyme which produces hydrogen peroxide [4]. Catalase is an enzyme responsible for further decomposition of the hydrogen peroxide to water and molecular oxygen. Hydroxyl radical ($\cdot OH$) is a product of hydrogen peroxide catalysis by ferrous ions, also referred as the Fenton Reaction. RNS include nitric oxide ($NO\bullet$) and peroxynitrite ($ONOO-$). Nitric oxide is produced by nitric oxide synthase (NOS) and peroxynitrite is a product of rapid reaction between ($NO\bullet$) and superoxide (O_2^-).

RONS can also be divided in the primary and secondary categories. Superoxide, hydrogen peroxide and nitric oxide belong to the primary group. They feature mechanisms capable of precise concentration controlling. Superoxide dismutase converts superoxide to hydrogen peroxide, which is further decomposed to water and oxygen by catalase. Various co-factors and Ca^{2+} calmodulin were found to be responsible for NOS activity and respective ($NO\bullet$) concentration control [5]. In addition to that, most reactions involving primary RONS are reversible, making them good candidates for signal transduction. Controlled production of ROS evolved as a part of immune system's defensive mechanisms and ROS destructive properties were utilized to damage the DNA of pathogenic bacteria.

In contrast, hydroxyl radical and peroxynitrite which belong to the secondary RONS are prone to irreversible bonds and lack of proper control mechanisms, making them potentially toxic and deleterious to a range of cellular machineries.

If so, then is it possible to prevent or mitigate the damage if detrimental processes are running loose? Or maybe the destructive power of ROS and RONS can be utilized for a good cause to induce apoptosis in cancerous cells? In order to answer these questions, a deeper understanding of ROS and

RONS metabolisms is required. This project seeks to address these questions and gain insight in the role of ROS in two different cell types.

To observe ROS-related metabolic mechanisms in response to chemical treatments, we have utilized ROS-sensitive fluorescent probes and confocal laser microscope.

Fluorescent probes react upon contact with ROS and RONS, increasing their fluorescencent yield up to 160-fold. Microscopy features distinct advantages over other fluorescent probe analytical methods like flow cytometry and microplate readers, as it is possible to evaluate additional parameters besides the fluorescence intensity by itself. Such advantages include the evaluation of the cell shape, mitochondrial fragmentation and localization of the fluorescent probe. Moreover, certain probes allow easy application of positive controls to the cells. However, this comes at the cost of more laborious workflow and data analysis.

Aims of the research

In this project we seek to understand the underlying mechanisms of ROS generation and its biological impact in hAMSC and one of their possible lineages, osteoblast-like MG-63 cells.

To reach this aim, we identified ROS generators in the cells and closely related metabolic pathways. By using various specific chemical treatments (e.g. Antioxidants, NOX inhibitors) we identified the sources and biological effects of intracellular ROS.

CHAPTER II: METHODS

Cell culture

Cell culture reagents and materials:

DMEM High Glucose solution, Fetal Bovine Serum (FBS), Phosphate Buffered Saline (PBS), Trypsin/EDTA solution (TE), L-Glutamine were supplied by Gibco™.
Cell culture growth medium consists of 89% DMEM, 10% FBS and 1% of L-Glutamine.

Cell culture seeding protocol:

1. Remove cell growth medium from the flask and wash twice with 10mL PBS.
2. Trypsinize the cells with 2 mL of 25% TE + 75% PBS mixture and incubate for 5 minutes at 37°C.
3. Gently shake the cell flask and inspect under the microscope if all the cells are detached
4. Stop the trypsinization process with 5ml of growth medium and collect the cells in Falcon tube.
5. Wash the cell culture flask with 10ml of growth medium and add the medium to Falcon tube.
6. Centrifuge at 1000 RPM for 5 minutes.
7. Remove the medium from the tube and resuspend the cell pellet in 2-5ml fresh medium
8. Estimate the amount of cells per 1mL of suspension (Cellometer or Neubauer chamber)
9. Fill a cell culture flask with growth medium and add required aliqout of cell suspension.
10. Prepare and distribute on the cell plate seeding solution consisting of growth medium and suspension based on 5000cells/cm^2 seeding density.
11. Gently shake and distribute the cells in the culture flask and the cell culture plate, incubate until desired confluence is reached.

Fluorescence probe staining medium:

For the cell imaging with laser scanning confocal microscopy, the use of Hank's Balanced Salt Solution (HBSS, supplied by Gibco™) is preferred over Dulbecco's Modified Eagle Medium (DMEM high glucose 4500mg/l, supplied by Gibco™) as the base for working solution preparation, as DMEM contains phenol red indicator which gradually changes its color upon exposure to the normal atmosphere conditions and respective pH changes which may interfere with the signal at certain frequencies. In this context and further, the solution consisting of the medium and fluorescencent dyes which gets applied and incubated together with cells is called the "Working solution".

DMSO

Dimethyl sulfoxide (DMSO) is an important substance with a broad variety of applications in cell research. It was used as cryoprotector in the cell culture applications (10% vol.), but its most important role is being solvent used to prepare stock and intermediary solutions for the molecular probes. It favors dissolution of the probe, protects it from oxygen and augments the proble entry inside the cell [6].

Most of the cell treatments (e.g. MitoTEMPO, DPI) also come in form of DMSO-based solution. However, upon reaching certain concentration, DMSO is known to exert toxic effects upon the cells. The response varies greatly based on cell type, exposure time and other experiment conditions. In this project, the mesenchymal stem cells were considered to specially sensitive to the DMSO concentration [7], therefore the concentration of DMSO was kept as low as possible (0,1% vol.). On the other hand, MG-63 osteosarcoma fibroblast-like cells are more robust and can withstand prolonged exposure to 0,5% vol. DMSO without noticeable deleterious effects.

Generalized staining protocol:

1. Working solution should be prepared in sufficient amounts based on the following rules:
• 2mL per well on the 2-well chamber slide and 1mL per well for the 4-well chamber slide.
• 4mL per well on the 6-well cell culture plate and 2mL per well on the 12-well cell culture plate.
2. The previous cell growth or treatment medium should be removed.
3. The cells should be washed with fresh medium (warmed up to 37°C) which matches the medium used for the working solution.
4. Working solution (warmed up to 37°C) should be added to the cells.
5. The cells submerged in the working solution should be incubated for at least 30 minutes. If the working solution is based on DMEM, then the cells should be incubated in an incubator which sustains the atmosphere with 5,0% CO_2 inside to avoid the pH changes and respectively, change in coloration of the phenol red indicator. Cells treated with HBSS-based working solution should be incubated in the incubator with normal atmospheric conditions.
*6. After the incubation process is over, the working solution should be removed, fresh and warmed up to 37°C medium added, then incubated for another 5 minutes.
*7. Medium should be removed, fresh and warmed up to 37°C medium added, now cells are ready for laser scanning microscope analysis.

Note: Steps 6 and 7 which include additional washing and incubation were utilized for human amnion mesenchymal stem cells stained with TMRM. Otherwise, they could lead to undesired signal degradation if other stains are utilized.

Fluorescent probes

Tetramethylrhodamine methyl ester (TMRM)

TMRM is a cell membrane-permeant probe which accumulates inside the mitochondrial matrix of a living cell. Accumulation of TMRM is proportional to the mitochondrial membrane potential $\Delta\psi$. Selective accumulation inside the mitochondria allows detailed examination of the $\Delta\psi$, mitochondria distribution across the cell, their fragmentation and overall condition of the cell (physiological or apoptotic). Healthy mitochondrial membrane potential is a hallmark of properly functioning electron transport chain, as it is generated by proton pumps of the mitochondrial membrane complexes I, III and IV [8].

The probe is supplied in powdered form (MW: 501g/mol) by PromoKine, and later stored in a form of 50mM DMSO stock solution at -25°C. The final concentration of TMRM in the working solution applied to cells should range between 10 – 500nM. Final concentration of 50nM was utilized for both cell types. The final volume of DMSO in solution results in 0,1% vol., assuming that no other probes or treatments are applied as well. Excitation laser wavelength of 543nm and emission wavelength filter range of 565 – 583nm were used.

TMRM working solution preparation protocol (1mL, 50nM):

1. Prepare intermediate DMSO-based 50µM solution from the 50mM storage stock solution (dilution factor 1000). This could be done by dissolving 1µL of 50mM storage stock solution in 999µL DMSO to produce 1mL of intermediary stock solution.

2. Prepare HBSS or DMEM medium based working solution with the TMRM concentration of 50nM from the intermediate 50µM DMSO solution (dilution factor 1000). This is achievable by dissolving 1µL of 50µM intermediate solution in 999µL HBSS or DMEM. Finally, the working solution should be warmed up to 37°C before application to the cells.
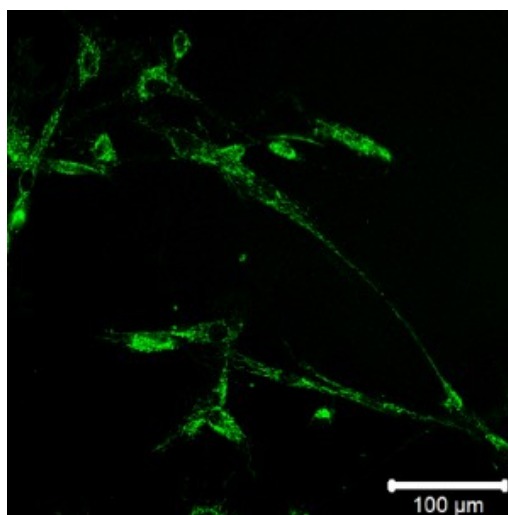
Figure 1. 50nM TMRM staining of hAMSC cells, total DMSO volume 0,1%

Chlormethyl derivative of 2',7'-Dichlorodihydrofluorescein diacetate (CM-H2DCFDA)

CM-H2DCFDA is a cell-permeant probe used as "General oxidative stress indicator" within the cell. Chlormethyl derivative of H2DCFDA features better retention in the living cells compared to H2DCFDA. It distributes evenly throughout the cytoplasm and transforms in its fluorescencent form upon contact with ROS. It is known to react to at least three types of ROS [9], hydrogen peroxide (H_2O_2), hydroxyl radical ($\cdot OH$) and peroxynitrite ($ONOO-$). This property can be used to easily establish a positive control by adding 100µM of hydrogen peroxide.

CM-H2DCFDA was supplied by ThermoFischer Scientific in powdered form (MW: 487g/mol) and was dissolved in DMSO to create a stock solution which is suitable for a short-term storage at -25°C for up a few hours. The probe are supplied in small vials, each containing 50µg of the substance. The suggested final concentration in the working solution should range between 1 and 10µM. For this project the final concentration of 10µM for MG-63 and 5µM for hAMSC were chosen. Excitation laser wavelength of 488nm and emission wavelength filter range of 505 – 638nm were used.

CM-H2DCFDA working solution preparation protocol (1mL, 10µM):

1. Dissolve the contents of the flask (50µg) in 8,7µL high-quality anhydrous DMSO to produce 10mM stock solution.
2. Dilute 1µL stock in 999µL HBSS (The use of medium which contains phenol red indicator is discouraged) to produce 10µM working solution with DMSO content of 0,1% vol.
Note: The cells could be washed after the incubation (30min at 37°C under normal atmosphere conditions in this project) to avoid background signal present in the medium. Otherwise, the conditions for incubations and final concentration in the working solution should be detected empirically.
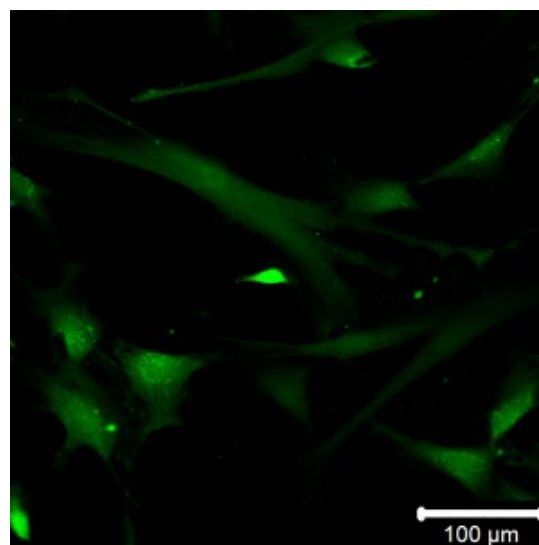
Figure 2. 5µM H2DCFDA staining of hAMSC cells, total DMSO volume 0,1%

4-amino-5-methylamino- 2',7'-difluorofluorescein diacetate - DAF-FM Diacetate

DAF-FM diacetate is compound used to detect and quantify nitric oxide (NO) signal molecule even at low concentrations (detection limit ~3nM) [10]. DAF-FM diacetate is essentially non-fluorescent until it comes in contact with NO to form highly fluorescent compound (approx. 160-fold increase).

The probe is also cell-permeant and passively diffuses through the cellular membranes, and does not have any specific accumulation preference inside the cell. DAF-FM diacetate is supplied by ThermoFischer Scientific in powdered form (MW: 496g/mol) and should be dissolved in DMSO to create a stock solution which is suitable for long-term storage at -25°C for up to six months. Repeated freezing and thawing is not recommended, therefore the probe should be stored in aliquots. The probes are supplied in small vials, each containing 50µg of the substance. The suggested final concentration in the working solution should range between 1 and 10µM.
Excitation laser wavelength of 488nm and emission wavelength filter range of 505 – 638nm were used.

DAF-FM working solution preparation protocol (1mL, 10µM):

1. Dissolve the contents of the flask (50µg DAF-FM diacetate) in 10µL high-quality anhydrous DMSO to produce 10mM stock solution.
2. Dilute 1µL stock in 999µL HBSS (Use of medium which contains phenol red indicator is discouraged) to produce 10µM working solution with DMSO content of 0,1% vol.
Note: The cells could be washed after the incubation (30min at 37°C in this project) to avoid background signal present in the medium. Otherwise, the conditions for incubations and final concentration in the working solution should be detected empirically.
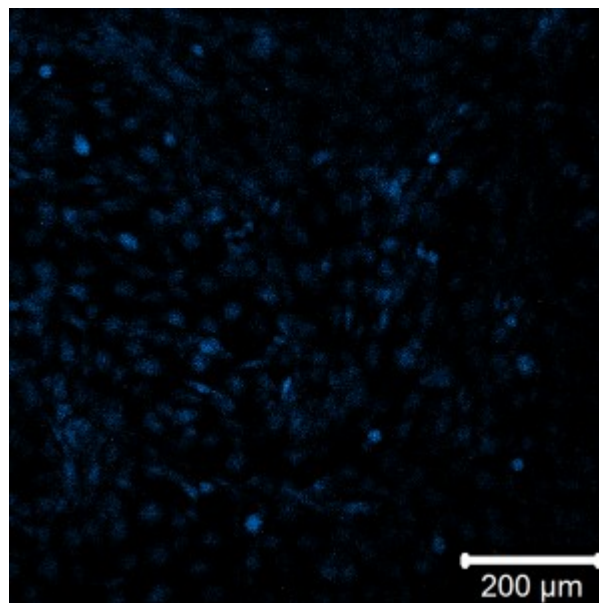
Figure 3. 10µM DAF-FM staining of MG-63 cells, total DMSO volume 0,1%

8

MitoSOX™ Red mitochondrial superoxide indicator for live cell imaging

MitoSOX™ is a cell membrane-permeant probe which is selectively oxidized by superoxide (O_2^-), but not other types of ROS [11]. The dye selectively targets living cell mitochondria which are a major source of superoxide production within the cell. The oxidation of the probe in the cytoplasmic space is partially prevented by superoxide dismutase. The probe also becomes highly fluorescent upon binding to the nucleic acids, therefore it should be used with caution. Respective excitation and emission maxima are 510 and 580nm.

MitoSOX™ is supplied by Thermofischer Scientific in a powdered form (MW: 759g/mol) and should be stable in powdered form for at least six months if stored properly at -25°C. The reagent should be dissolved in DMSO to make a stock solution. The produced stock solution is not suitable for long-term storage and should be used as soon as possible. The probes are supplied in small vials, each containing 50µg of the substance. The recommended final concentration of MitoSOX™ in the working solution should not exceed 5µM to avoid excessive nuclear staining. Excitation laser wavelength of 488nm and emission wavelength filter range of 574 – 617nm were used.

MitoSOX™ working solution preparation protocol (1mL, 5µM):

1. Dissolve the contents of the vial (50µg MitoSOX™) in 16µL high-quality anhydrous DMSO to produce 5mM stock solution.
2. Dilute 1µL stock in 999µL HBSS (Recommended buffer in the product information) to produce 5µM working solution with DMSO content of 0,1% vol.
Note: The cells could be washed after the incubation (15min at 37°C in this project) to avoid background signal present in the medium. Unlike most probes, shorter incubation time is recommended to reduce nuclear staining.
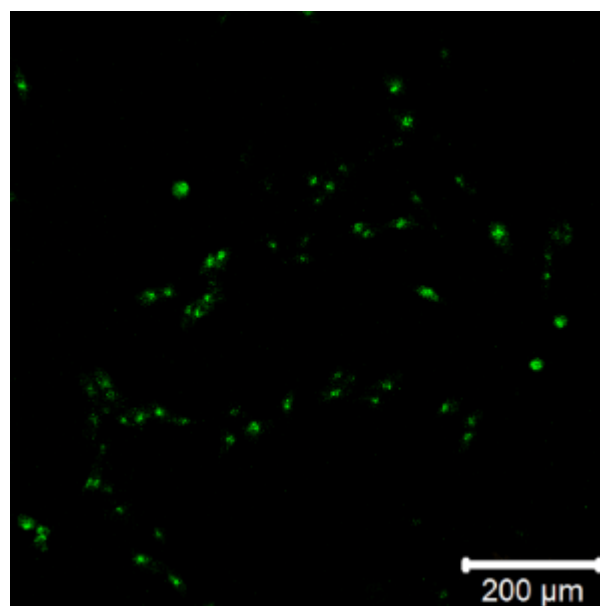
Figure 4. 5µM MitoSOX™ staining of MG-63 cells, total DMSO volume 0,1%

MitoTracker™ DeepRed FM

Deep Red FM is a cell membrane-permeant probe which is selectively accumulated inside the mitochondria of a living cell based on their membrane potential. The probe targets active mitochondria, and therefore could be used to determine their localization. However, once the Deep Red FM probe had entered mitochondria it steadily fixates inside and will not leave them. For comparison, TMRM is readily washed out from the mitochondria if the reduction or loss of the mitochondrial membrane potential occurs. Therefore, Deep Red FM should be used with caution as an indicator of mitochondrial membrane potential. The hallmark of Deep Red FM are specific excitation and emission maxima of 644 and 665nm, which lie deep in the red part of the spectrum. This property facilitates the use of Deep Red FM together with other probes, as their spectra are very unlikely to overlap.

MitoTracker™ Deep Red FM is supplied by Thermofischer Scientific in a powdered form (MW: 544g/mol). The reagent should be dissolved in DMSO to make a stock solution which is suitable for storage for up to six months at -25°C. The probes are supplied in small vials, each containing 50µg of the substance. The recommended final concentration of Deep Red FM in the working solution should range between 20 and 500nM. In this project the concentration of 50nM was utilized. Excitation laser wavelength of 633nm and emission wavelength filter range of 654 – 688nm were used.

Deep Red FM working solution preparation protocol (1mL, 50nM):

1. Dissolve the contents of the vial (50µg) in 10,8µL high-quality anhydrous DMSO to produce 10mM stock solution.
2. Dilute 1µL stock in 199µL DMSO to produce 50 µM Deep Red FM intermediate solution.
3. Dilute 1µL intermediate solution in 999µL HBSS to produce 50nM working solution
Note: The cells could be washed after the incubation (30min at 37°C in this project) to avoid background signal present in the medium.
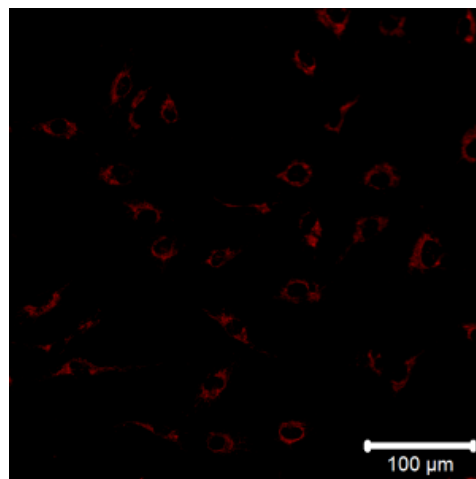
Figure 5. 50nM DeepRed FM staining of HUVEC cells, total DMSO volume 0,1%

MitoTracker™ Red CM-H2Xros

CM-H2Xros is a cell membrane-permeant probe which fluoresces upon oxidation. The dye selectively targets living cell mitochondria and accumulates depending on mitochondrial membrane potential. Unlike MitoSOX™, H2Xros is not marketed to oxidize selectively on contact with superoxide (O_2^-) but upon contact with ROS in general. However, it is known that mitochondria primarily produce superoxide, part of which is transformed to hydrogen peroxide via mitochondrial superoxide dismutase[12], which theoretically can also react with the probe. However, the addition of hydrogen peroxide control (100 μM) did not affect the CM-H2Xros signal in MG-63 cells, so the conclusion that CM-H2Xros is selective to superoxide was drawn.

CM-H2Xros is supplied by Thermofischer Scientific in a powdered form (MW: 497g/mol) and should be stable in powdered form for at least six months if stored properly at -25°C. The reagent should be dissolved in DMSO to make a stock solution. The produced stock solution is not suitable for long-term storage and should be used as soon as possible. The probes are supplied in small vials, each containing 50μg of the substance. The general guideline recommendation regarding final concentration of CM-H2Xros in the working solution should not exceed 500nM. However, in the MG-63 cell line even the maximum recommended concentration did not produce any results, so the concentration of 5μM was used instead. The possibility to use 5μM concentration of CM-H2Xros was supported in the literature[13].

CM-H2Xros 5μM working solution preparation protocol (1mL, 5μM):

1. Dissolve the contents of the vial (50μg CM-H2Xros) in 20,1μL high-quality anhydrous DMSO to produce 5mM stock solution.
2. Dilute 1μL stock in 999μL HBSS (Recommended buffer in the product information) to produce 5μM working solution with DMSO content of 0,1% vol.
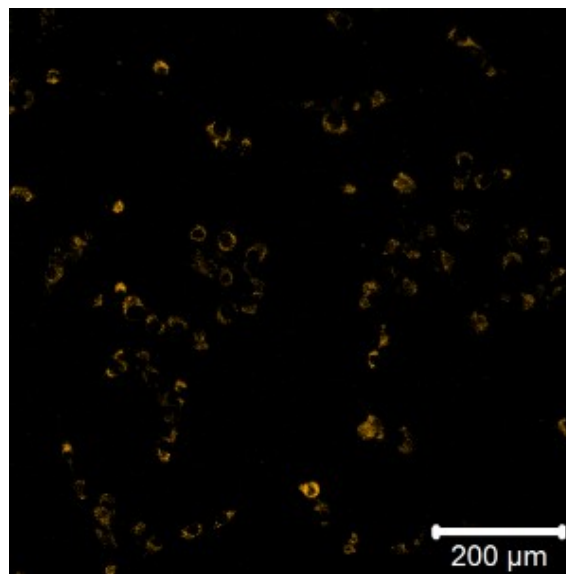
Figure 6. 5μM CM-H2Xros staining of MG-63 cells, total DMSO volume 0,1%

Analytics and data processing

For the image acquisition we utilized Zeiss LSM 510-META confocal laser scanning microscope with settings adjusted according to individual fluorescencent probe specifications described above. We used 20x magnification objectives for hAMSC and 10x for MG-63 cell analysis.
The Zeiss ZEN software package was utilized for primary image processing (e.g. background threshold settings, ROI selection).

The basic threshold setting for the background was set at 2. By selecting the ROI comprised of individual cells we extracted the averaged fluorescence values after chemical treatment and in the control group.
The data was exported in form of tables for further processing.
We used MEDCALC® software to calculate the statistics, including the p-value and Graphpad Prism 8 to create the figures.

CHAPTER III: RESULTS

hAMSC results

Reflected amnion human amnion stem cells (hAMSC) were exposed to 8 different treatments which were reported in the literature to influence ROS levels within the cells for 24 hours. Cellular ROS levels were measured with H2DCFDA fluorescent probe and mitochondrial membrane potential (Δψm) was assessed with TMRM. We applied the following treatments: NOX inhibitors, antioxidants and an iron chelator Desferal. NOX inhibitors included apocynin and DPI. Antioxidants include SOD, Catalase, Mannitol, MitoTEMPO and Thiourea. Experiments were carried out in 4 rounds. MitoTEMPO experiments were carried out in 2 rounds in addition to the rest of the treatment groups and were compared with respective fresh DMSO 0,1% controls (ROI [N] = 14). DPI 20µM experiments were carried out separately in 2 rounds with respective DMSO controls (ROI [N] = 25).

Nr.	Treatment	ROI amount [N]	Final concentration [µM; U/mL]
1	DMSO Control	44	0,1% vol
2	Apocynin	46	50µM
3	Catalase	46	300 U/mL
4	SOD	42	200 U/mL
5	DPI	46	5µM
6	DPI	16	20µM
7	Mannitol	47	50000µM
8	Thiourea	44	30000µM
9	Desferal	46	100µM
10	MitoTEMPO	14	1µM

Table 1: hAMSC 24h treatment group table.

Nr.	Treatment	TMRM (Δψm)	H2DCFDA (Cellular ROS)
1	DMSO Control		
2	Apocynin	↑ +14%*	↑ +24%
3	Catalase	↓ - 15%	↑ +10%
4	SOD	↓ - 15%	↑ +11%
5	DPI 5µM	↑ +28%***	↓ -59%***
6	DPI 20µM	↑ +9%*	↓ -55%***
7	Mannitol	↑ +2%	↓ -15%
8	Thiourea	↓ -1%	↓ -9%
9	Desferal	↑ +21%**	↓ -29%*
10	MitoTEMPO	↑ +1%	↓ -33%*

Table 2: hAMSC result table. Statistically significant ($p < 0,05$) observations are marked with single asterisk, very significant observations ($p < 0,01$) with double asterisk and observations ($p < 0,001$) with triple asterisk. P-values are two-tailed and compared to the respective DMSO control groups.

hAMSC apocynin 24h treatment

hAMSC were exposed to 50µM concentration of NADPH oxidase inhibitor apocynin for 24 hours. 50µM apocynin treated group image analytics consists of 46 ROI data, and 44 ROI data was taken respective control group. The background signal cut-off threshold was set at 2, and hAMSC with 0,1% vol. DMSO added were taken as control groups. Results on the graphs are represented as average fluorescence value of the treatment group + standard deviation, p-values were determined by two-tailed t-test.
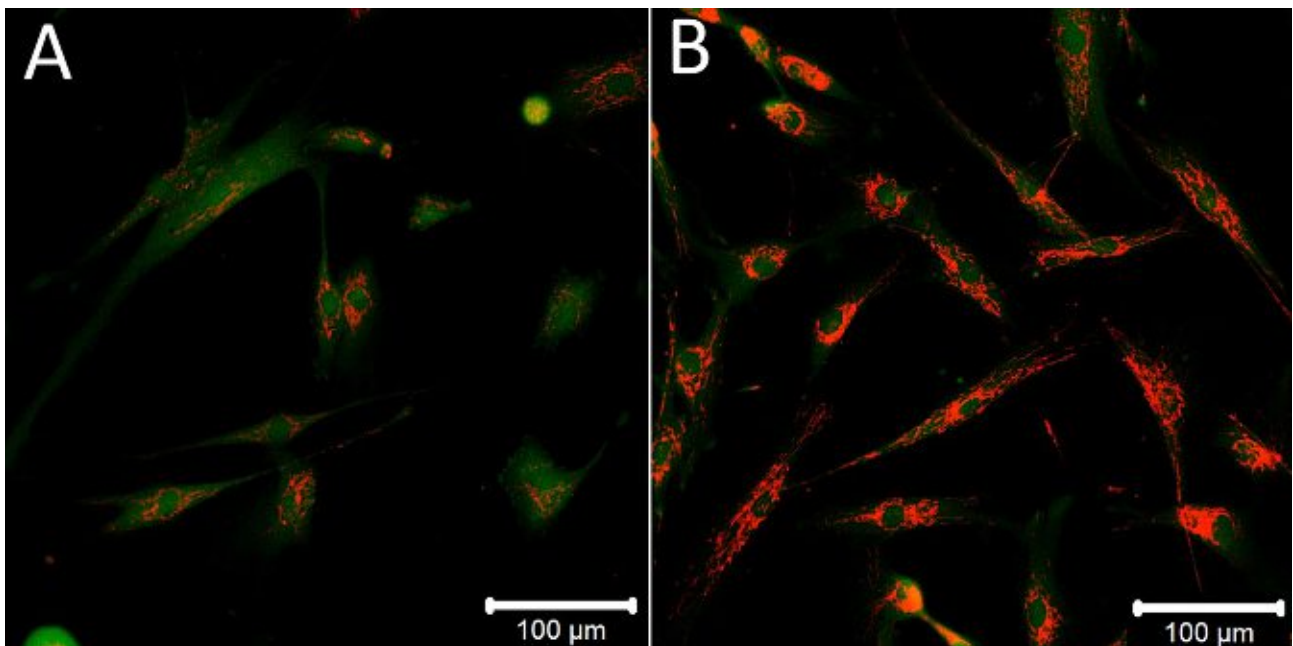
Figure 7. LSM image examples. A: hAMSC control group with 0,1% vol. DMSO, 24h incubation. B: hAMSC 50µM apocynin treatment group, 24h incubation. 50nM TMRM, 5µM H2DCFDA probes.

hAMSC 50µM Apocynin treatment (24h)
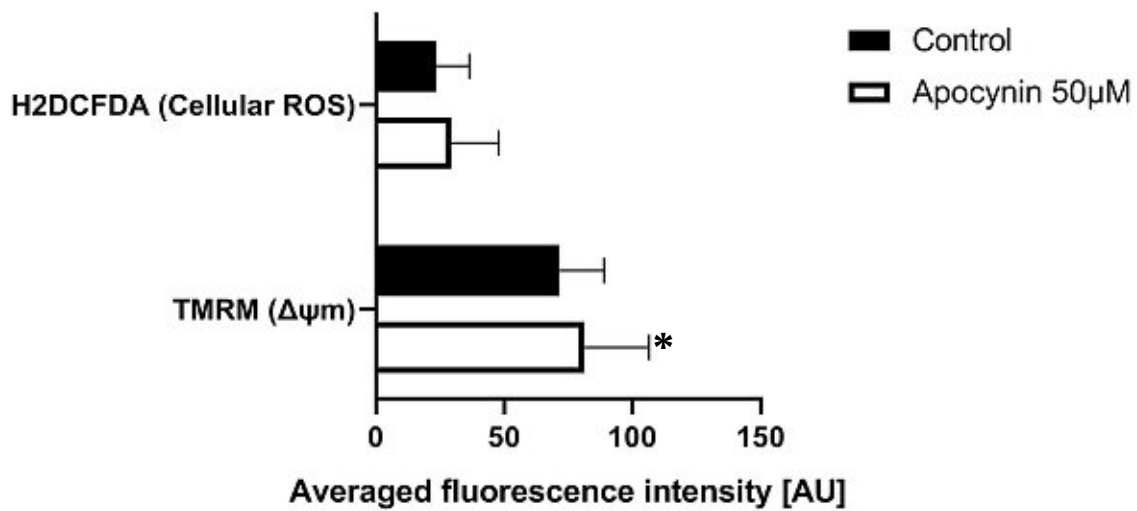
Figure 8. Measurement of cellular ROS and Δψm levels in hAMSC after 24h apocynin 50µM treatment. Statistically significant change of TMRM (p = 0,0343) is observable. H2DCFDA signal change is statistically insignificant (p = 0,0923).

hAMSC catalase 24h treatment

hAMSC were exposed to 300 U/mL concentration of enzymatic antioxidant catalase for 24 hours. Catalase treated group image analytics consists of 46 ROI data, and 44 ROI data was taken respective control group. The background signal cut-off threshold was set at 2, and hAMSC with 0,1% vol. DMSO added were taken as control groups. Results on the graphs are represented as average fluorescence value of the treatment group + standard deviation, p-values were determined by two-tailed t-test.
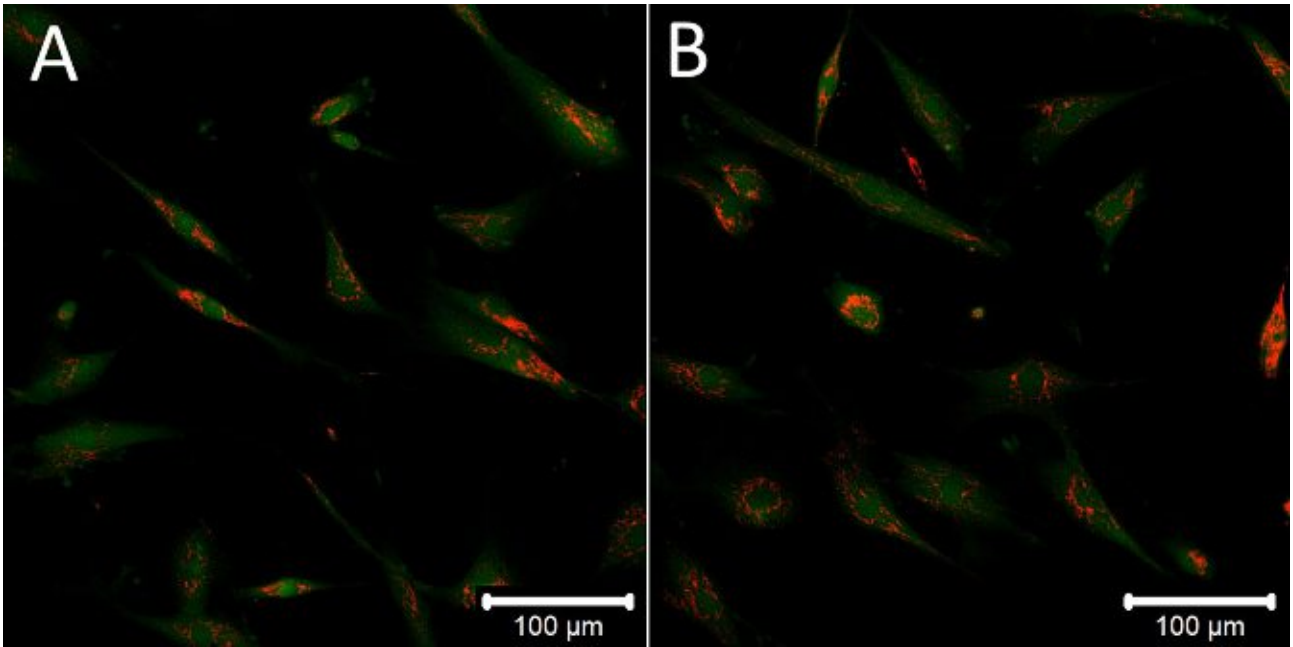
Figure 9. LSM image examples. A: hAMSC control group with 0,1% vol. DMSO, 24h incubation. B: hAMSC cell 300 U/mL catalase treatment group, 24h incubation. 50nM TMRM, 5µM H2DCFDA probes.
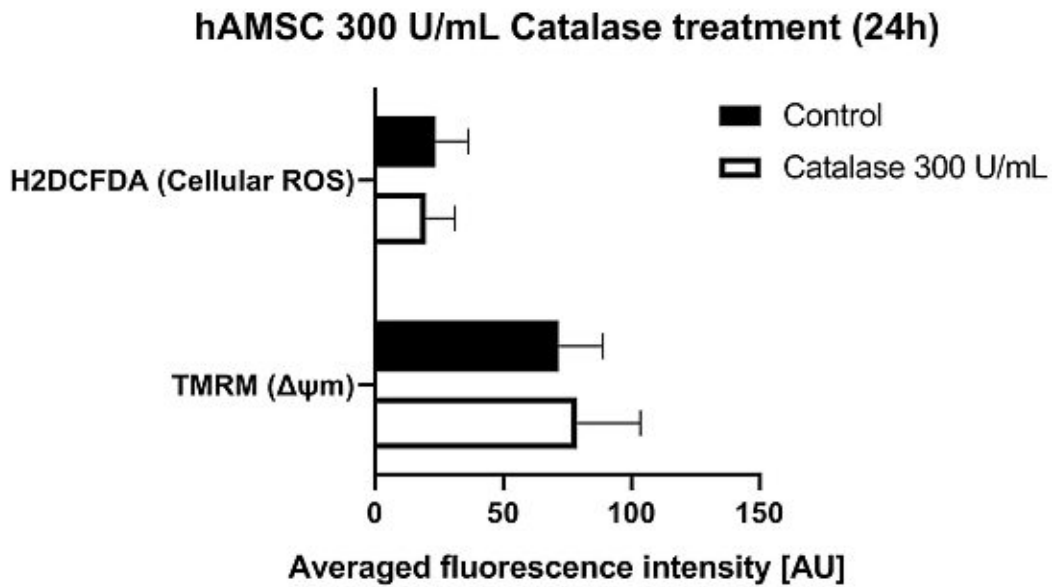
Figure 10. Measurement of cellular ROS and $\Delta\psi$m levels in hAMSC after 24h catalase 300 U/mL treatment. No statistically significant signal changes were observed in TMRM (p = 0,1080) and H2DCFDA (p = 0,1696).

hAMSC SOD 24h treatment

hAMSC were exposed to 200 U/mL concentration of enzymatic antioxidant SOD for 24 hours. SOD treated group image analytics consists of 42 ROI data, and 44 ROI data was taken respective control group. The background signal cut-off threshold was set at 2, and hAMSC with 0,1% vol. DMSO added were taken as control groups. Results on the graphs are represented as average fluorescence value of the treatment group + standard deviation, p-values were determined by two-tailed t-test.
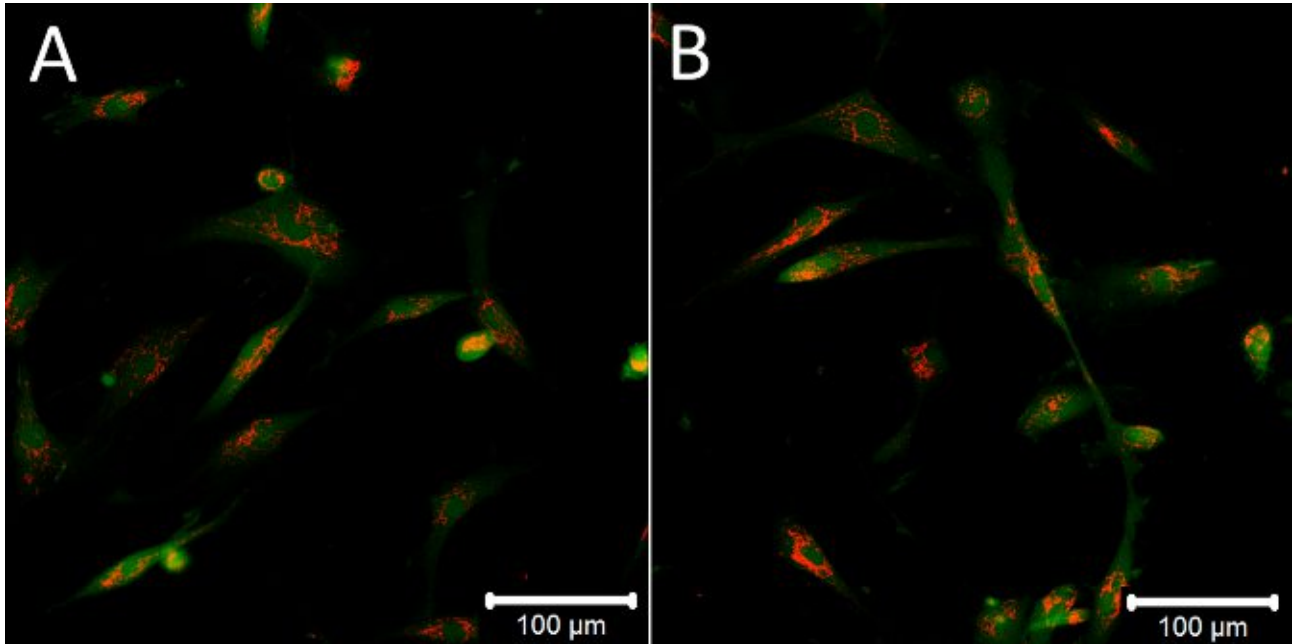
Figure 11. LSM image examples. A: hAMSC control group with 0,1% vol. DMSO, 24h incubation. B: hAMSC 200 U/mL SOD treatment group, 24h incubation. 50nM TMRM, 5µM H2DCFDA probes.

hAMSC 200 U/mL SOD treatment (24h)
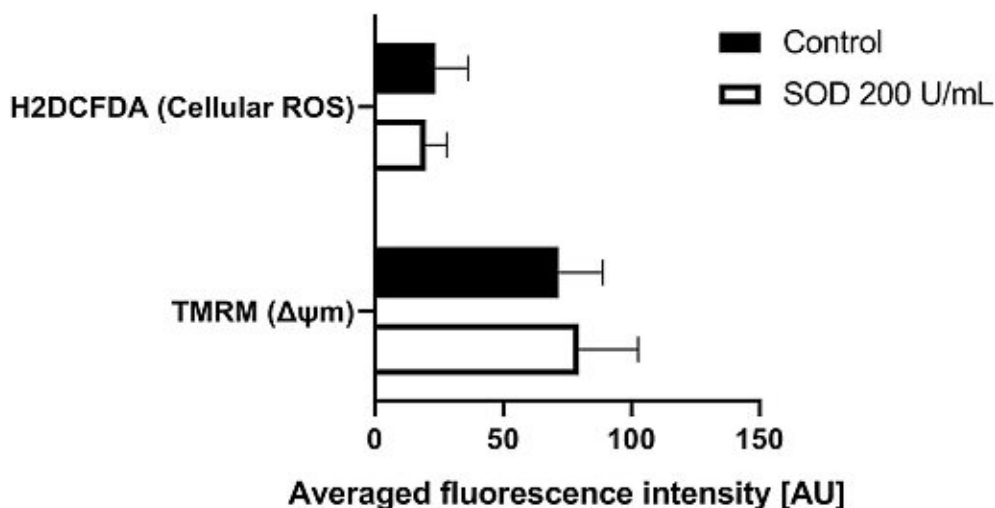
Figure 12. Measurement of cellular ROS and Δψm levels in hAMSC after 24h SOD 300 U/mL treatment. No statistically significant signal changes were observed in TMRM (p = 0,0754) and H2DCFDA (p = 0,1211).

hAMSC DPI 24h treatments

hAMSC were exposed to 20µM and 5µM concentration of NADPH oxidase inhibitor DPI for 24 hours. DPI 20µM treated group image analytics consists of 16 ROI data, and 44 ROI data was taken respective control group. The background signal cut-off threshold was set at 2, and hAMSC with 0,1% vol. DMSO added were taken as control groups. Results on the graphs are represented as average fluorescence value of the treatment group + standard deviation, p-values were determined by two-tailed t-test.
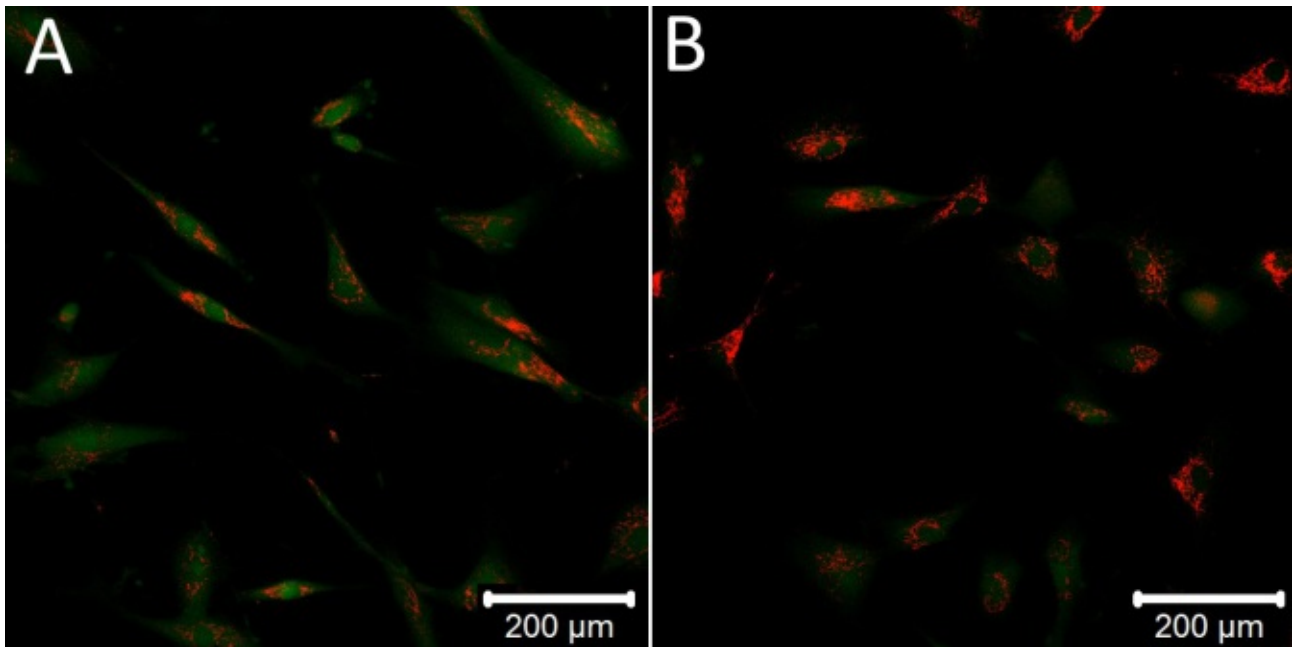
Figure 13. LSM image examples. A: hAMSC control group with 0,1% vol. DMSO, 24h incubation. B: hAMSC cell 20µM DPI treatment group, 24h incubation. 50nM TMRM, 5µM H2DCFDA probes.
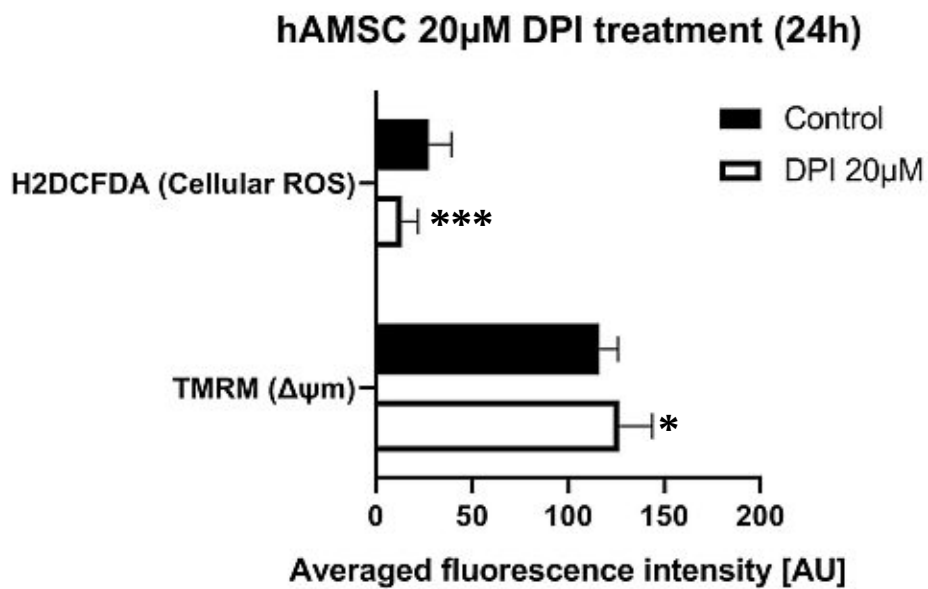
Figure 14. Measurement of cellular ROS and Δψm levels in hAMSC after 24 hours of DPI 20µM treatment. Statistically significant increase in TMRM (p = 0,0226) and decrease in H2DCFDA (p = 0,0002) signals were observed.
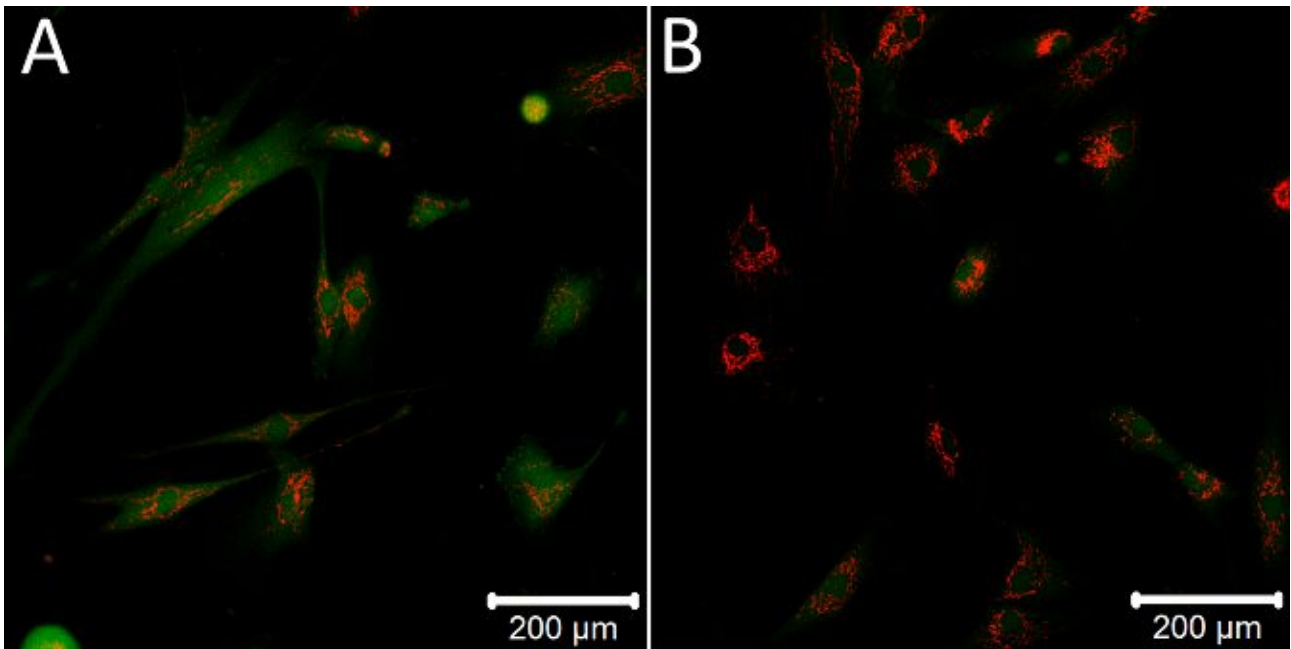
Figure 15. LSM image examples. A: hAMSC control group with 0,1% vol. DMSO, 24h incubation.
B: hAMSC cell 5µM DPI treatment group, 24h incubation. 50nM TMRM, 5µM H2DCFDA probes.
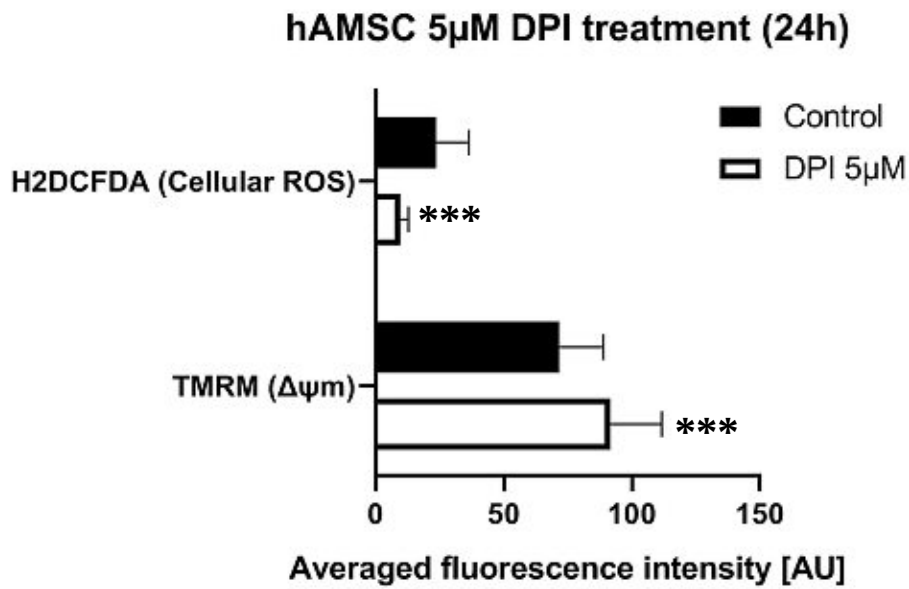
Figure 16. Measurement of cellular ROS and $\Delta\psi$m levels in hAMSC after 24h DPI 5µM treatment.
Statistically significant increase of TMRM (p = 0,0001) and decrease in H2DCFDA
(p < 0,0001) signals were observed.

20

hAMSC mannitol 24h treatment

hAMSC were exposed to 50mM concentration of sugar alcohol mannitol with ROS scavenging properties for 24 hours. Mannitol treated group image analytics consists of 47 ROI data, and 44 ROI data was taken respective control group. The background signal cut-off threshold was set at 2, and hAMSC with 0,1% vol. DMSO added were taken as control groups. Results on the graphs are represented as average fluorescence value of the treatment group + standard deviation, p-values were determined by two-tailed t-test.
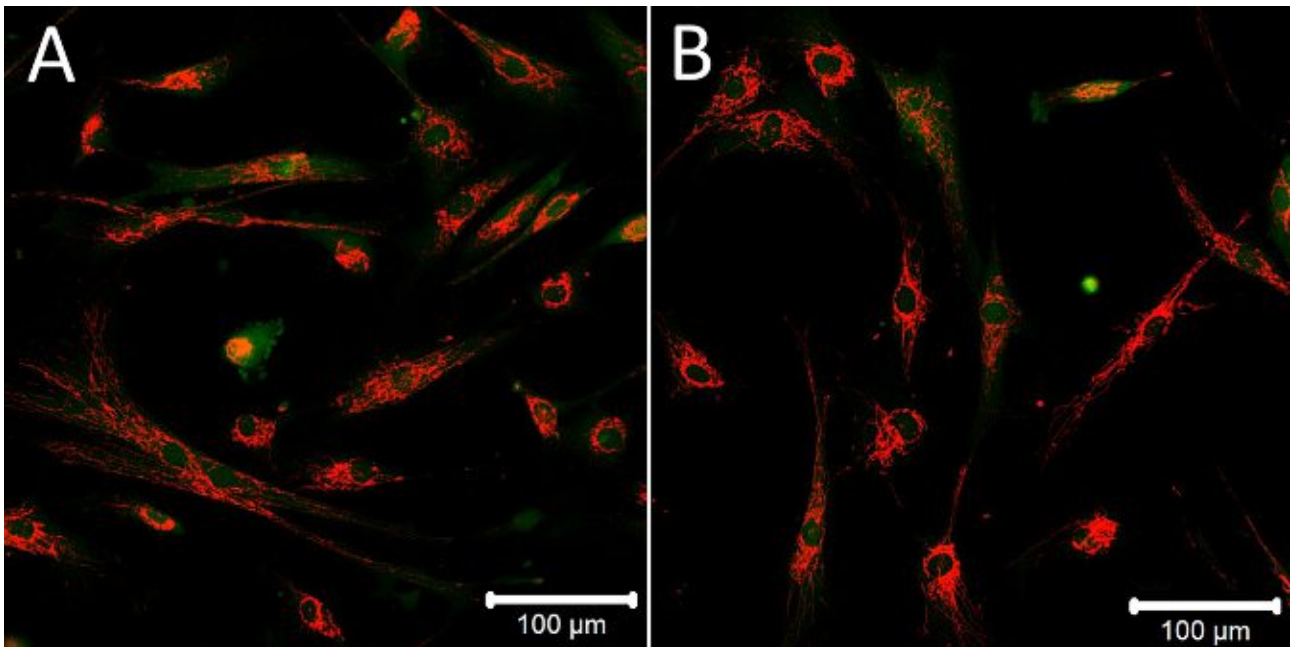
Figure 17. LSM image examples. A: hAMSC control group with 0,1% vol. DMSO, 24h incubation. B: hAMSC 50mM mannitol treatment group, 24h incubation. 50nM TMRM, 5μM H2DCFDA probes.

hAMSC 50 mM Mannitol treatment (24h)
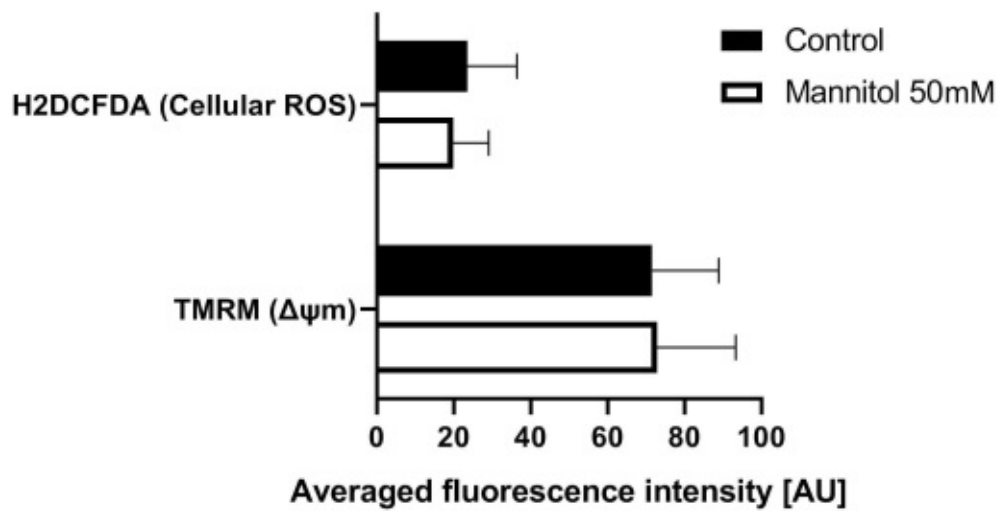
Figure 18. Measurement of cellular ROS and Δψm levels in hAMSC after 24h mannitol 50mM treatment. No statistically significant signal changes were observed in TMRM (p = 0,7558) and H2DCFDA (p = 0,1234).

hAMSC thiourea 24h treatment

hAMSC were exposed to 30mM concentration of thiourea ROS scavenger for 24 hours. Thiourea treated group image analytics consists of 44 ROI data, and 44 ROI data was taken respective control group. The background signal cut-off threshold was set at 2, and hAMSC with 0,1% vol. DMSO added were taken as control groups. Results on the graphs are represented as average fluorescence value of the treatment group + standard deviation, p-values were determined by two-tailed t-test.
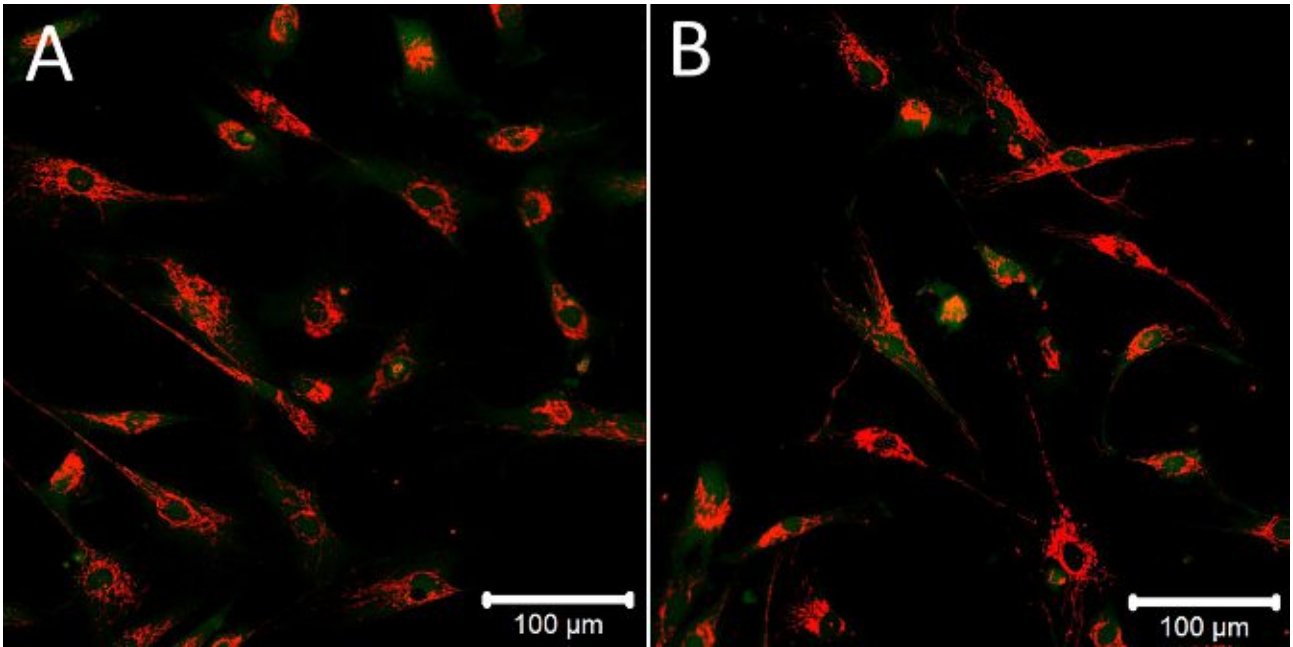
Figure 19. LSM image examples. A: hAMSC control group with 0,1% vol. DMSO, 24h incubation. B: hAMSC 30mM thiourea treatment group, 24h incubation. 50nM TMRM, 5μM H2DCFDA probes.
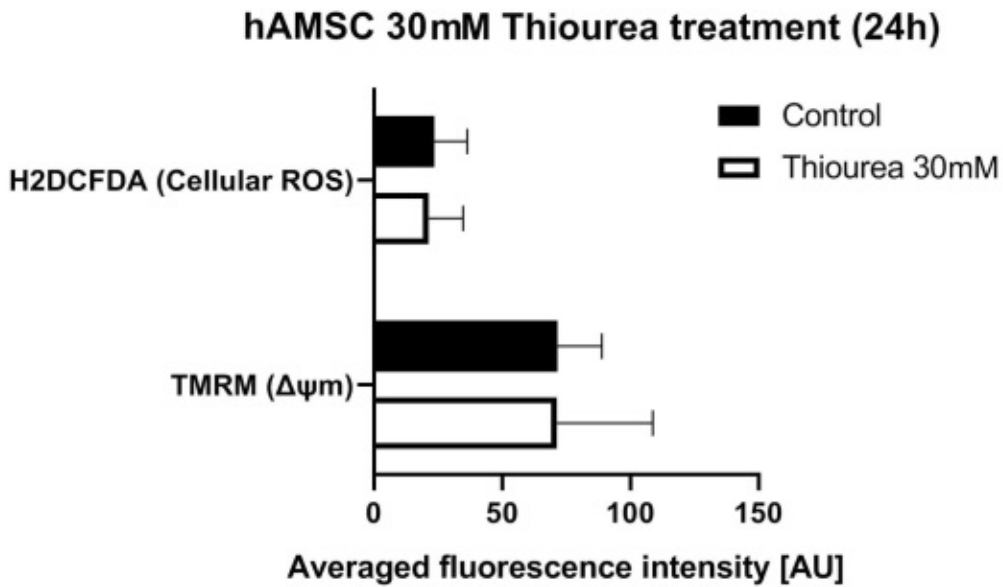
Figure 20. Measurement of cellular ROS and $\Delta\psi$m levels in hAMSC after 24h thiourea 30mM treatment. No statistically significant signal changes were observed in TMRM (p = 0,9759) and H2DCFDA (p = 0,4585).

hAMSC desferal 24h treatment

hAMSC were exposed to 100µM concentration of iron chelator desferal for 24 hours. Desferal treated group image analytics consists of 46 ROI data, and 44 ROI data was taken respective control group. The background signal cut-off threshold was set at 2, and hAMSC with 0,1% vol. DMSO added were taken as control groups. Results on the graphs are represented as average fluorescence value of the treatment group + standard deviation, p-values were determined by two-tailed t-test.
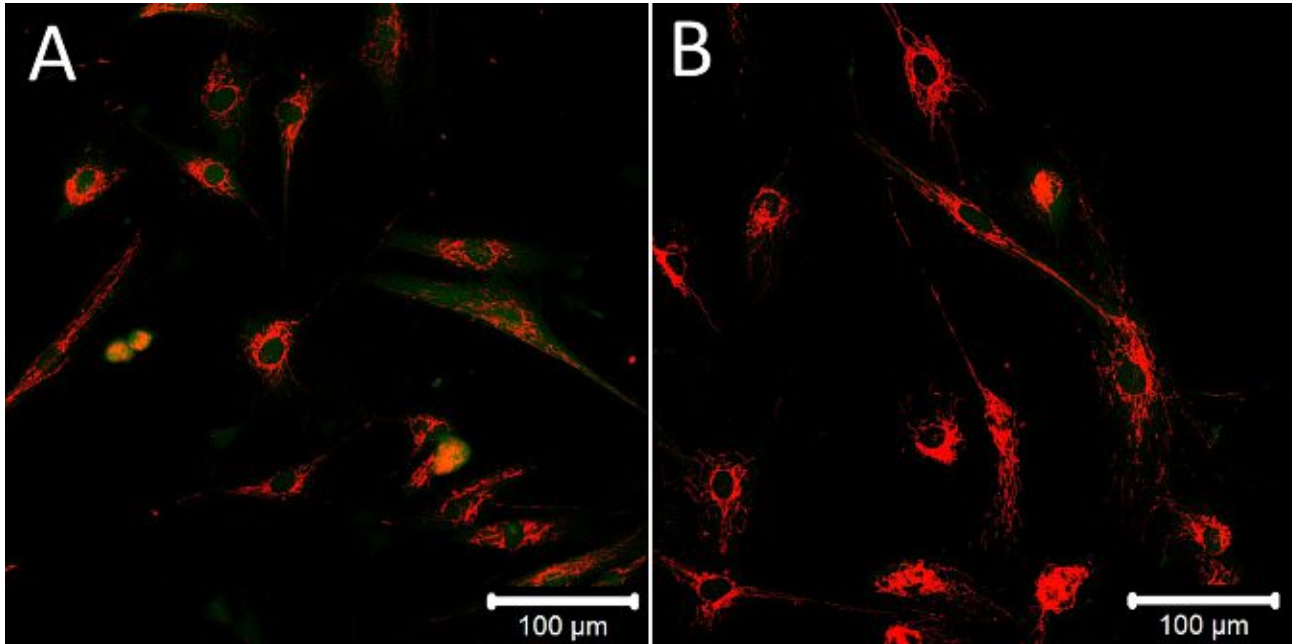
Figure 21. LSM image examples. A: hAMSC control group with 0,1% vol. DMSO, 24h incubation. B: hAMSC 100µM desferal treatment group, 24h incubation. 50nM TMRM, 5µM H2DCFDA probes.

hAMSC 100µM Desferal treatment (24h)
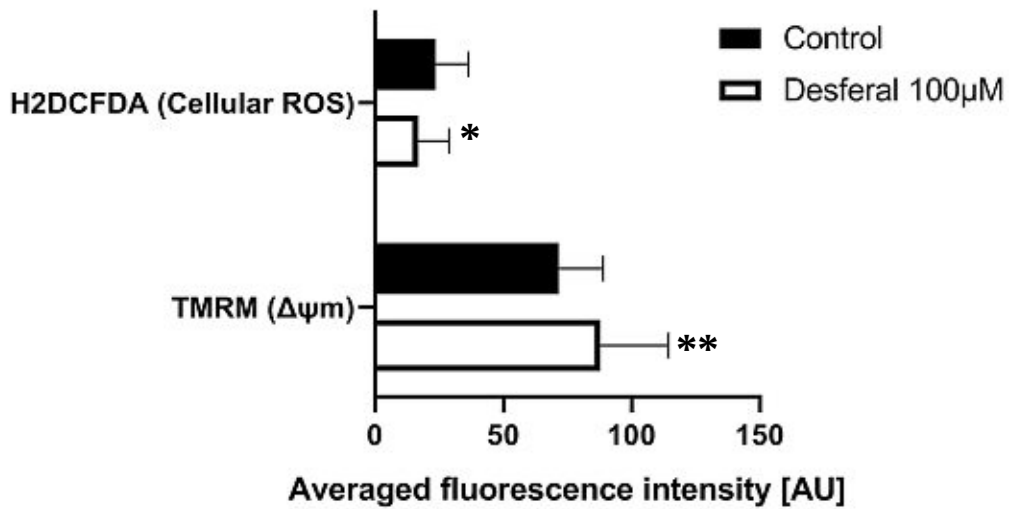
Figure 22. Measurement of cellular ROS and Δψm levels in hAMSC after 24h 100µM desferal treatment. Statistically significant increase of TMRM (p = 0,0011) and decrease in H2DCFDA (p = 0,012) signals were observed.

hAMSC MitoTEMPO 24h treatment

hAMSC were exposed to 1µM concentration of mitochondrial antioxidant MitoTEMPO for 24 hours. MitoTEMPO treated group image analytics consists of 25 ROI data, and 25 ROI data was taken respective control group. The background signal cut-off threshold was set at 2, and hAMSC with 0,1% vol. DMSO added were taken as control groups. Results on the graphs are represented as average fluorescence value of the treatment group + standard deviation, p-values were determined by two-tailed t-test.
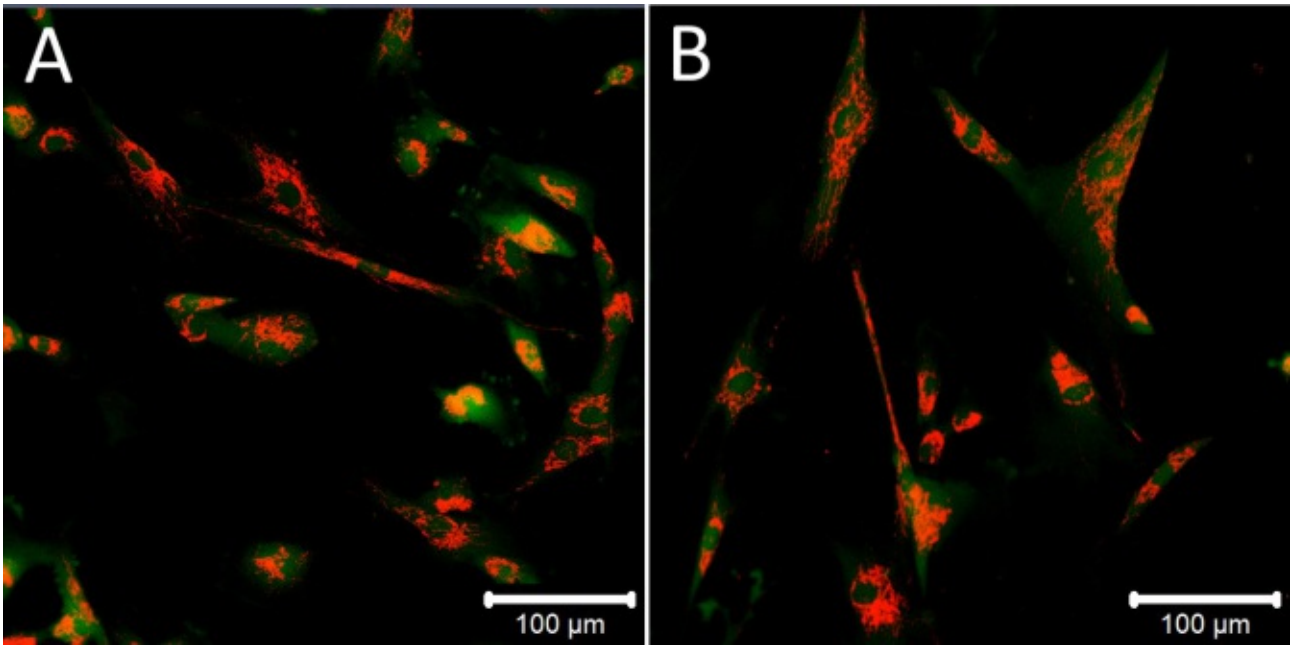
Figure 23. LSM image examples. A: hAMSC control group with 0,1% vol. DMSO, 24h incubation. B: hAMSC 1µM MitoTEMPO treatment group, 24h incubation. 50nM TMRM, 5µM H2DCFDA probes.
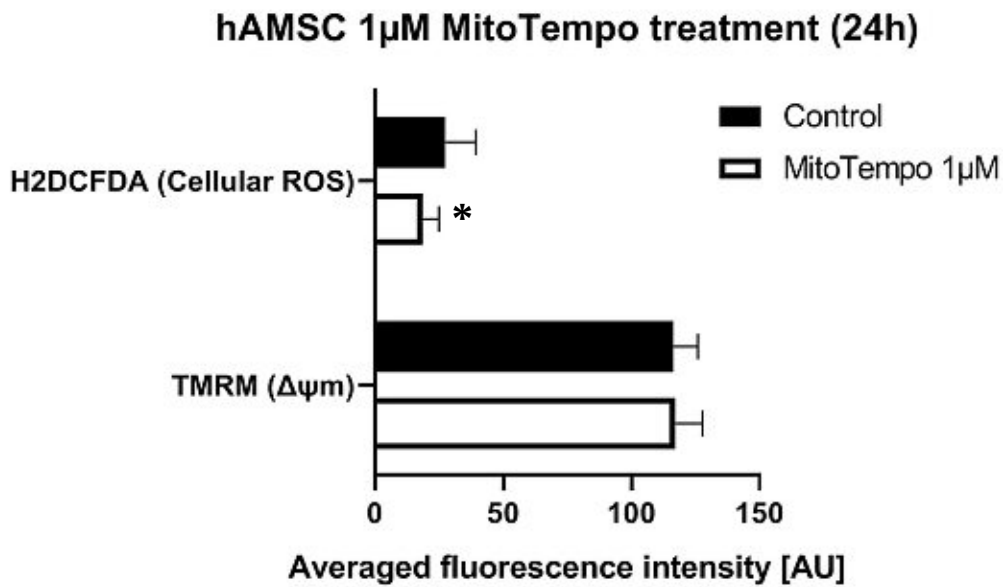
Figure 24. Measurement of cellular ROS and $\Delta\psi$m levels in hAMSC after 24h MitoTEMPO 1µM treatment. No statistically significant signal changes were observed in TMRM ($p = 0,8235$), but statistically significant H2DCFDA signal alterations were detected ($p = 0,0194$).

hAMSC result overview

NADPH Oxidase inhibitor apocynin (50µM) failed to induce any statistically significant effect on ROS production in hAMSC. It has been reported that no NOX inhibitory effect can often be found in cells not involved in immune response [14]. A slight but statistically significant increase in Δψm was also observed.

Catalase is an enzyme which catalyses hydrogen peroxide decomposition to water and molecular oxygen, but It did not affect both Δψm and cellular ROS levels. Catalase is a relatively big protein (60kDA) which might not be able pass the cellular membrane in substantial amounts, so its action could be limited [15].

Similarly to catalase, SOD ability to catalyze superoxide to hydrogen peroxide can be mostly limited to the extracellular space due to its weight (32,5kDA). This can explain the lack of effect on mitochondrial membrane potential and cellular ROS.

NOX inhibitor DPI treatment at both 5µM and 20µM concentration caused an anticipated effect of cellular ROS reduction. Increase in Δψm was also observed for both concentrations.

Mannitol was reported to be capable of ROS scavenger properties [16], however no statistically significant effect on Δψm and cytoplasm ROS were observed. Mannitol has been reported to be a non-permeating molecule, so its mode of action is most probably limited to extracellular space [17].

Thiourea is an organosulfuric compound known for its ROS scavenging properties [18], however it failed to induce any effects on hAMSC. It could be explained by the polarity of the molecule and not being able to pass through the cellular membrane.

Desferal is an iron chelator which captures Fe^{2+} ion, thus preventing Fenton reaction which produces toxic hydroxyl radical from hydrogen peroxide ($Fe^{2+} + H_2O_2 = Fe^{3+} + \cdot OH + OH^-$). H2DCFDA is capable of hydroxyl radical detection, so the cellular ROS signal reduction can be explained with Fenton reaction inhibition by desferal. An increase of Δψm was observed as well.

Observation of mitochondrial antioxidant MitoTEMPO revealed a decrease of cellular ROS levels, but it no statistically significant changes in Δψm were observed.

In short, out of 8 treatment groups only 3 behaved in the way it was anticipated. However, there is a body of literature providing an explanation why efficacy of the rest of the treatments was limited. Based on the results the following conclusions can be made:

1. NOX is expressed in hAMSC cells and it can be inhibited by DPI. This suggests predominant expression of NOX4 isoform, as it is typically located on the endoplasmic reticulum [19] and produces ROS in the cytoplasm, unlike the other isoforms producing ROS in the extracellular space.

2. Toxic hydroxyl radical (·OH) is present in hAMSC cells and its formation can be quenched by iron chelator Desferal.

3. Mitochondria are also contributing to the ROS levels in cytoplasm. Mitochondrial SOD mimetic MitoTEMPO reduced ROS levels in the cytoplasm by removing superoxide in the mitochondria. Otherwise, mitochondrial superoxide is catalyzed by mitochondrial SOD enzyme to hydrogen peroxide and permeates through the membrane in the cytoplasm.

MG-63 results

MG-63 DPI and MitoTEMPO treatment

MG-63 were exposed to 10µM concentration of NOX inhibitor DPI for 24 hours. DPI treated group image analytics consists of 25 ROI data, and 25 ROI data was taken respective control group. The background signal cut-off threshold was set at 2, and MG-63 cells with 0,05% vol. DMSO added were taken as control groups. Results on the graphs are represented as average fluorescence value of the treatment group + standard deviation, p-values were determined by two-tailed t-test.
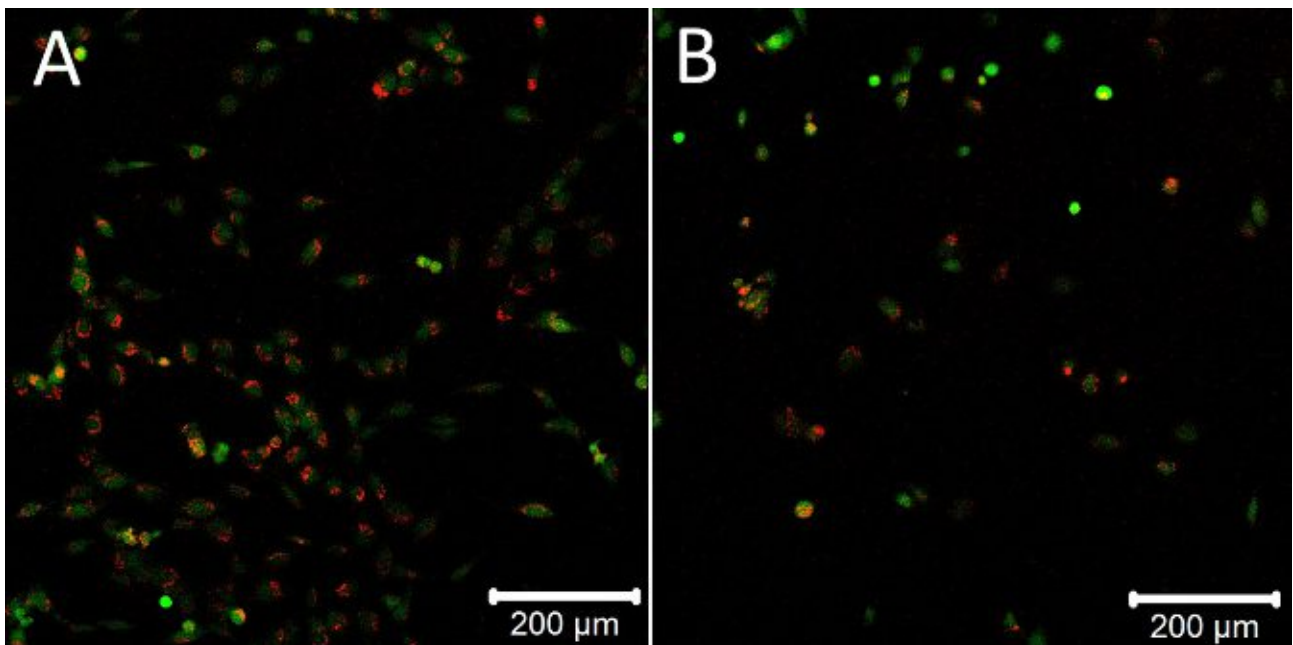
Figure 25. LSM image examples. A: MG-63 control group with 0,05% vol. DMSO, 24h incubation. B: MG-63 10µM DPI treatment group, 24h incubation. 50nM TMRM, 10µM H2DCFDA probes.

MG-63 10µM DPI treatment (24h)
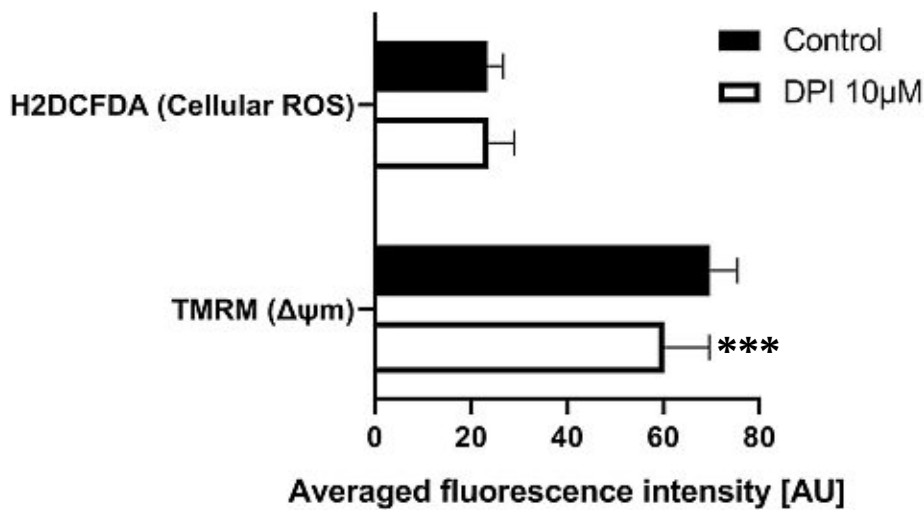
Figure 26. Measurement of cellular ROS and Δψm levels in MG-63 cells after 24h DPI 10µM treatment. Statistically significant signal changes were observed in TMRM (p = 0,0001), no statistically significant H2DCFDA signal alterations were detected (p = 0,7685).

Since no effect on cellular ROS was observed, a decision to increase DPI concentration to 100µM was made. However, after 24h incubation with 100µM DPI the MG-63 had lost the capability to adhere to the bottom of the glass and were washed away during the fluorescent probe staining procedure, so no suitable cells for analysis were found. Looking at the Fig. 25 (DPI 10µM treatment of MG-63 cells) it is noticeable that DPI likely affects the proliferation of MG-63 cells, something which was not directly observable in hAMSC cell images. Therefore, the incubation time with 100µM DPI was reduced to 30 minutes to observe effects more directly. Control group DMSO [ROI [N] = 15] volume was adjusted to 0,5% to match 100µM DPI group [ROI [N] = 15].
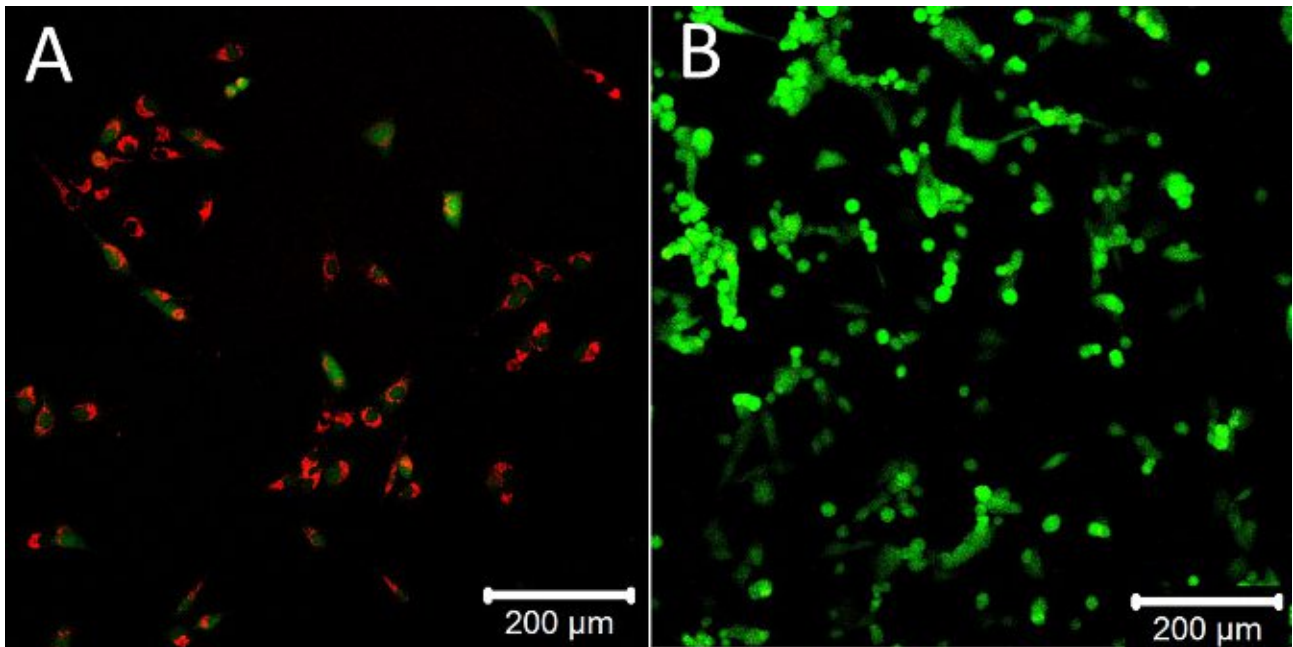
Figure 27. LSM image examples. A: MG-63 control group with 0,5% vol. DMSO, 30min incubation. B: MG-63 100µM DPI treatment group, 30 min incubation. 50nM TMRM, 10µM H2DCFDA probes.
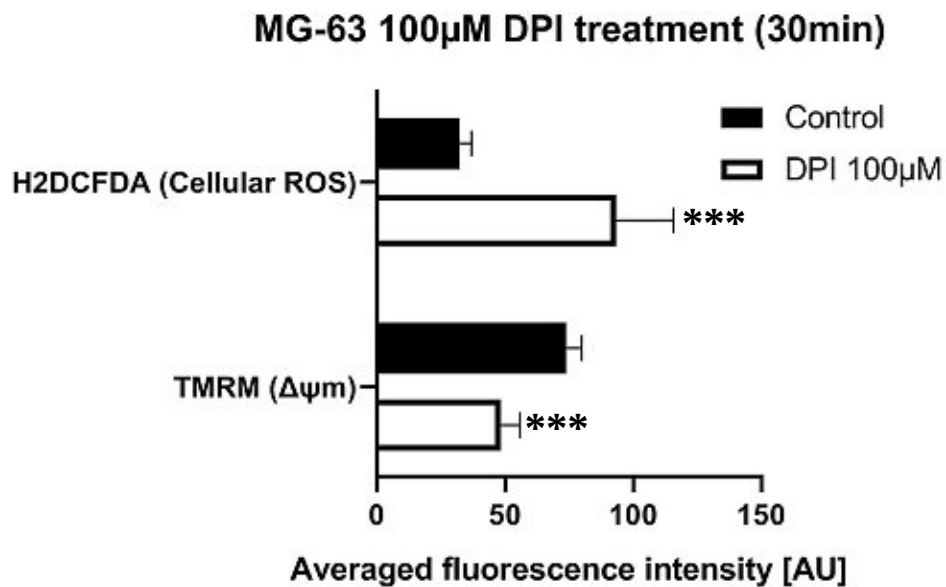
Figure 28. Measurement of cellular ROS and Δψm levels in MG-63 cells after 30min DPI 100µM treatment. Statistically significant signal changes were observed in TMRM ($p < 0,0001$), statistically significant H2DCFDA signal alterations were detected ($p < 0,0001$).

Paradoxically, treatment with 100µM DPI NOX inhibitor which exhibited antioxidant properties in hAMSC cells at lower concentration induced almost 3-fold increase of cellular ROS. TMRM signal and respective Δψm have decreased considerably as well.

In order to identify the origin of the massive ROS spike, a combined treatment of mitochondrial antioxidant MitoTEMPO (20µM) concentration and 100µM DPI was tested. At first, a MitoTEMPO 20µM application alone for 30 minutes was tested to find if there is an observable effect by itself. The analysis included 15 ROI for MitoTEMPO and DMSO control 0,25% vol. group.

MG-63 20µM MitoTempo treatment (30min)
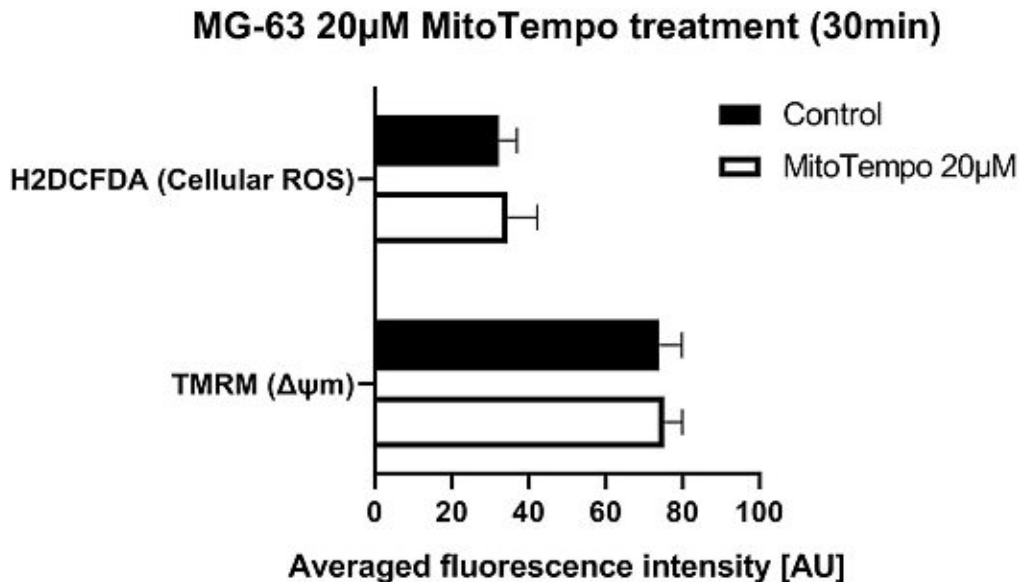
Figure 29. Measurement of cellular ROS and Δψm levels in MG-63 cells after 30min MitoTEMPO 20µM treatment. No statistically significant signal changes were observed in TMRM ($p = 0,4959$) and H2DCFDA signal ($p = 0,3139$).

It was found that application of 20µM MitoTEMPO alone did not cause any statistically significant impact by its own, so it would facilitate easier result interpretation.

In order to avoid DMSO overload on the MG-63 cells, at first the cells were pre-treated with 20µM concentration of MitoTEMPO for 30 minutes, thoroughly washed and then 100µM DPI was applied for 30 minutes.

Respective negative control group was treated with 0,25% vol. DMSO for 30 minutes, thoroughly washed, and then 0,5% vol. DMSO added for another 30 minutes. Similarly, 100µM DPI group was taken as a positive control, incubated with 0,25%vol. DMSO for 30 minutes, washed and then 100µM DPI added. All 3 group data consists of 15 ROI analysis.
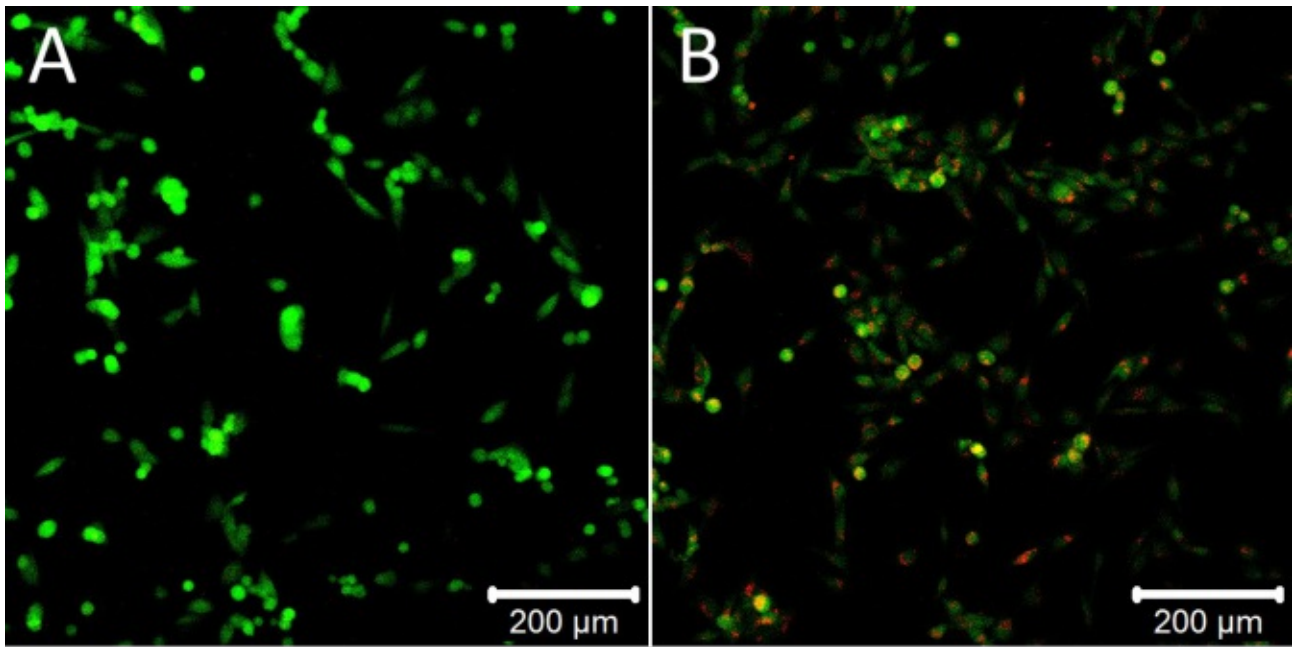
Figure 30. LSM image examples. A: MG-63 100µM DPI group, 30+30min incubation. B: MG-63 20µM MitoTEMPO + 100µM DPI treatment group, 30+30 min incubation. 50nM TMRM, 10µM H2DCFDA probes.
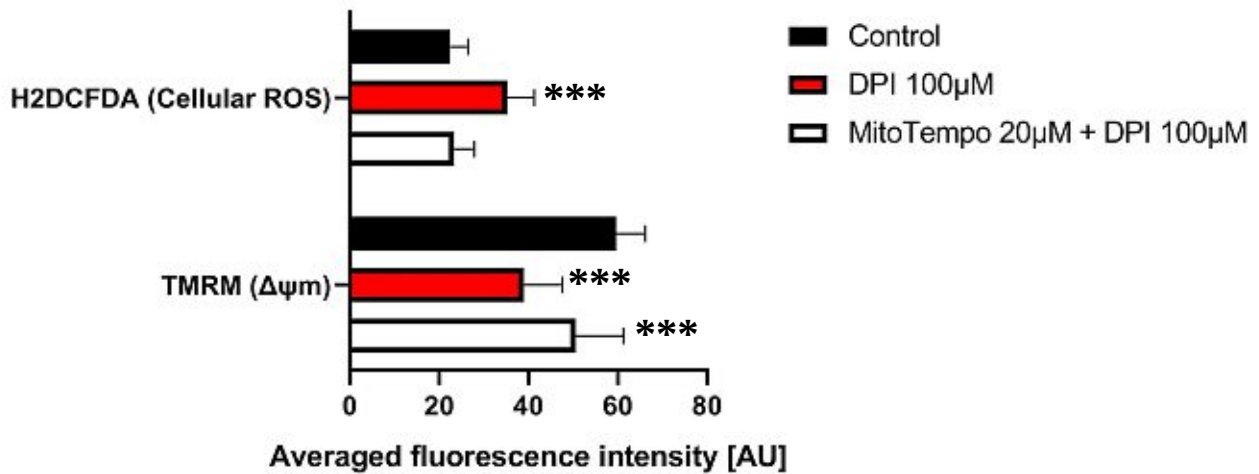
Figure 31. Measurement of cellular ROS and Δψm levels in MG-63 cells after 30min 20µM MitoTEMPO + 100µM DPI treatment. DPI group cellular ROS signal difference is very significant (p < 0,0001). TMRM measurements of Δψm in DPI and MitoTEMPO+DPI group are very significantly different from control (p < 0,001).

Overall, administration of 20µM mitochondrial antioxidant MitoTEMPO mitigated the impact of 100µM DPI treatment on the cellular ROS levels, and partially reduced the effect on Δψm. This provides a clue that the cytoplasm ROS burst induced by 100µM DPI treatment is of mitochondrial origin.

To gain more evidence to support this interpretation, 100µM DPI experiment was repeated with MitoTracker™ Red CM-H2Xros probe, which specifically targets and detects mitochondrial ROS.
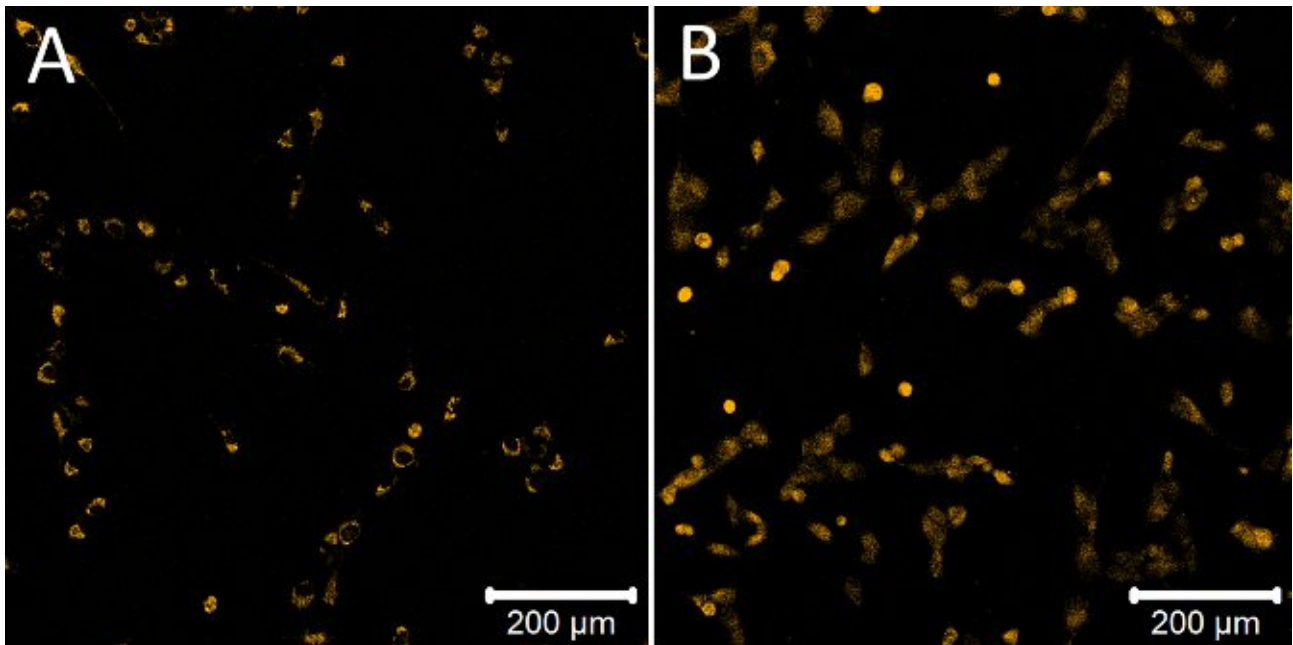
Figure 32. LSM image examples. A: MG-63 control group with 0,5% vol. DMSO, 30min incubation. B: MG-63 100µM DPI treatment group, 30 min incubation. 5µM H2Xros probe.

H2Xros in control group shows distinct mitochondrial localization of the fluorescent probe (Figure 32. A), and application of 100µM DPI treatment had caused a distinct change of localization and migration to the cytoplasmic space (Figure 32. B). This supports the idea of mitochondrial origin of the ROS spike.

However, this rises the question whether the measured cytoplasmic ROS is mostly hydrogen peroxide, or the superoxide is still present. In order to test it, MitoSOX™ Red Mitochondrial Superoxide Indicator probe was used. However, MitoSOX is known to cause nuclear staining, so the pixels with maximal fluorescence intensity (255) were excluded in addition to the background threshold value of 2. The control group analysis included 10 ROI, and 100µM DPI treatment group consisted of 18 ROI.
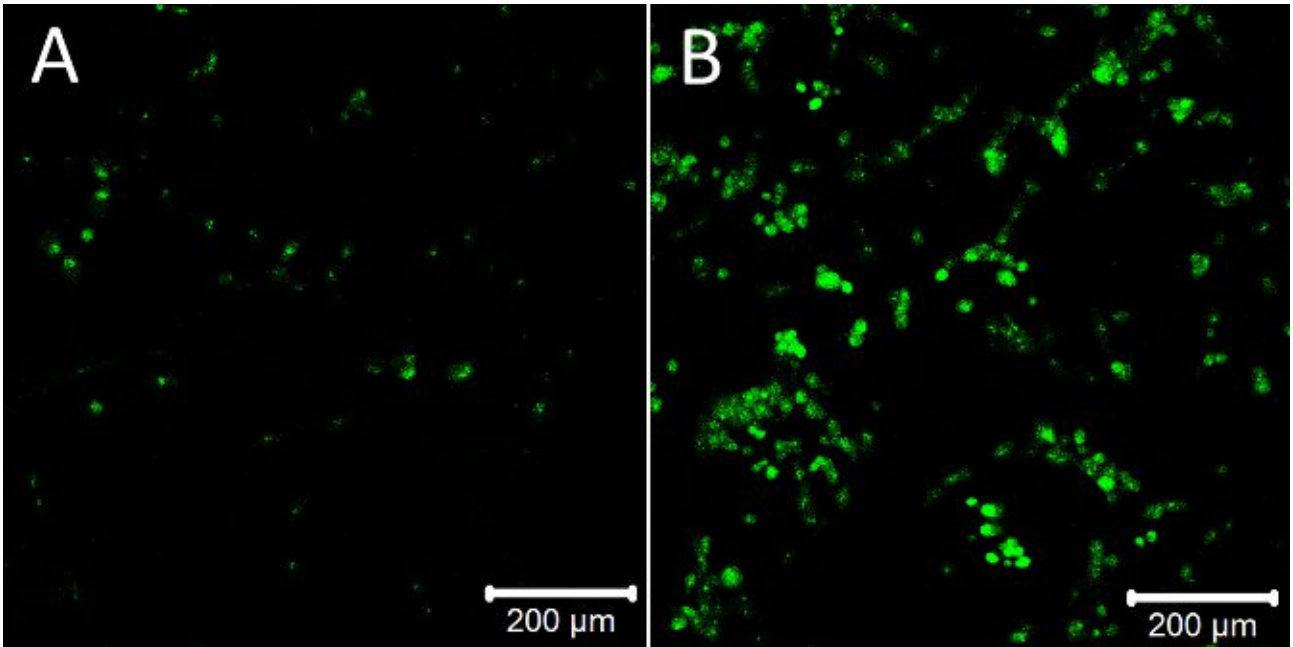
Figure 33. LSM image examples. A: MG-63 control group with 0,5% vol. DMSO, 30min incubation. B: MG-63 100µM DPI treatment group, 30 min incubation. 5µM MitoSOX™ probe.
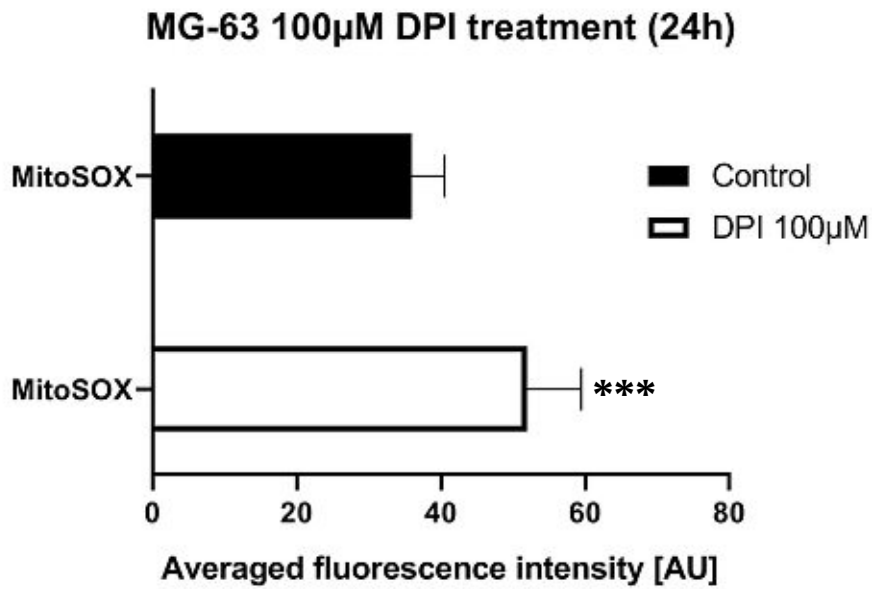
Figure 34. Measurement of superoxide levels in MG-63 cells after 30min 100µM DPI treatment. Statistically significant signal change was observed ($p < 0,0001$).

The results support the idea that the ROS leaving mitochondria after 100µM DPI application does not get fully catalyzed to hydrogen peroxide by SOD, and the superoxide is still present in the cytoplasm. This leads to a potential of toxic peroxynitrite formation if nitric oxide signal molecule is present ($NO + O_2^- = ONOO-$). The presence of nitric oxide in MG-63 cells can be confirmed by application of DAF-FM Diacetate stain.
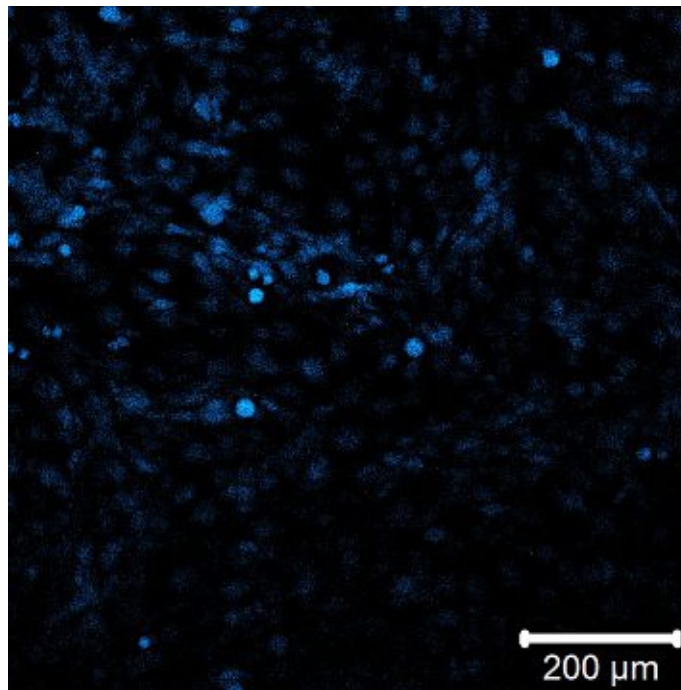
Figure 35. LSM image example. MG-63 stained with DAF, 0,1% DMSO vol. 5µM DAF-FM probe.

The presence of DAF signal indicates that NO and nitric oxide synthase are present in MG-63 cells. Once the cells are exposed to 100µM DPI and ROS spike occurs, formation of peroxynitrite is possible.

Increase of ROS levels are known to cause mitochondrial transition permeability pore opening [20], and this is the likely mechanism how the change of ROS localization occurs upon exposure to 100µM DPI.

hAMSC and MG-63 result summary

Overall, the following conclusions can be made:

1. Treatment with comparable concentration of NOX inhibitor DPI (10µM) does not exert the same effect of cellular ROS level reduction on MG-63 cells as it does on hAMSC. This happens most probably due to a different NOX isoform expression in MG-63 cells.

2. Treatment with high DPI concentrations (100µM) induces an opposite effect of cellular ROS spike and oxidative stress, compared to conventional use of DPI for its antioxidant-like function.

3. Mitochondria are the source of the ROS burst induced by 100µM DPI. These ROS are presented in a form of superoxide which was confirmed with MitoSOX probe. ROS likely enters cytoplasm through mitochondrial transition pore opening induced by elevated mitochondrial ROS levels.

4. Once in the cytoplasm, part of the mitochondrial ROS can be converted to hydrogen peroxide via SOD and toxic peroxynitrite by reacting with nitric oxide.

5. Possibility of peroxynitrite formation was confirmed by innate nitric oxide presence in MG-63 cells, however distinguishing between peroxynitrite and hydrogen peroxide is difficult as H2DCFDA probe is highly sensitive to both peroxynitrite and hydrogen peroxide [21].

CHAPTER IV: DISCUSSION

Metabolic pathways of ROS in hAMSC

ROS generated by NOX

In the majority of cells the NOX is located in cytoplasmic membrane and releases ROS in a form of superoxide in the extracellular environment. It has been shown that the ROS released from NOX can diffuse to cytoplasm and contribute to intracellular signaling. To test whether such mechanism occurs in hAMSC we examined effect of NOX inhibitors, on the levels of cytoplasmic ROS.

Indeed, we observed that inhibition of NOX reduced the amount of cytoplasmic ROS upon treatment with DPI. Both 5µM and 20µM DPI caused significant decrease (-59% and -55%, respectively; $p < 0,001$) in H2DCFDA signal. Another NOX – inhibitor, apocynin, did not have any remarkable effect. The latter is in line with previous publications, showing that apocynin is effective predominantly in phagocytic cells [22].

To prove that the ROS generated by NOX are released in the medium we examined effects of extracellular ROS scavengers, SOD and catalase, on the levels of cytoplasmic ROS.

However, neither SOD nor catalase had an effect on cytoplasmic levels of ROS.

This result suggests that NOX occurring in hAMSC releases ROS directly into cytoplasm rather than in the medium. It is known that NOX4 is the only isoform situated in the endoplasmic reticulum and produces ROS in the intracellular space. Therefore our data suggest that NOX4 is at least one of the major sources of cytoplasmic ROS.

As already mentioned earlier, the efficacy of NOX inhibitor apocynin is very limited in the investigated cell type and the produced results can neither support nor reject our theory.

Mitochondria may be injured by excessive amount of intracellular ROS. To test whether there is such interplay between cytoplasmic ROS and mitochondrial function we determined mitochondrial membrane potential upon treatment with DPI.

We observed that DPI not only decreased ROS levels in cytoplasm, but also elevated mitochondrial membrane potential. We observed statistically significant increase in mitochondrial membrane potential in both 5µM DPI group (+29%; $p < 0,01$) and in 20µM DPI group (+9%; $p < 0,05$).

We assume that the increase in $\Delta\psi m$ might be due to ROS mediated crosstalk between NOX and mitochondria, namely ROS generated by NOX damage mitochondria causing a decrease in $\Delta\psi m$, while inhibition of NOX by DPI reduces ROS levels and elevates $\Delta\psi m$; this mechanism is in line

with previously published data and it has already been shown that generation of mitochondrial ROS correlates positively with an increase of Δψm [23]. Negative correlation observed in our experiment suggests that cytoplasmic ROS do not originate from mitochondria. On the other hand, an increase of Δψm was observed as well. To investigate this matter further, we examined generation of mitochondrial ROS.

ROS generated by mitochondria in hAMSC

Another important source of intracellular ROS is the electron transport chain of mitochondria. Mitochondria generate superoxide radical which forms hydrogen peroxide via disproportionation reaction or by mitochondrial SOD. Hydrogen peroxide, which is considered as a normal product of mitochondrial respiration can relatively freely permeate through mitochondrial membrane into the cytoplasmic space [24]. Mitochondrial superoxide is the primary mitochondrial ROS antioxidants such as MitoTEMPO. The next question we addressed was whether mitochondrial supeoxide contributes to intracellular pool of ROS.

Treatment with 1μM MitoTEMPO for 24 hours resulted in statistically significant H2DCFDA signal reduction (-33%; p < 0,05). No impact on Δψm was observed.

In this experiment we have observed that MitoTEMPO successfully scavenged superoxide produced by mitochondria, leaving less superoxide available for mitochondrial SOD causing consequently a decrease of hydrogen peroxide levels in cytoplasm. However there is an alternative mechanism explaining this phenomenon. It has been shown that low levels mitochondrial ROS can regulate the activity of NOX generating high concentrations of ROS. Thus, reduced amount of cytoplasmic ROS in response to mitoTEMPO can be due to a decrease in NOX activity.

However, since H2DCFDA probe is sensitive not only to hydrogen peroxide, but also hydroxyl radicals we have investigated this possibility with iron chelator Desferal.

Hydroxyl radicals in hAMSC

Hydroxyl radicals ($\cdot$OH) are highly reactive ROS produced via Fenton reaction in biological systems in presence of ferrous ions and hydrogen peroxide. ($Fe^{2+}+H_2O_2 \rightarrow Fe^{3+}+(\cdot OH)$).

Previous NOX and mitochondrial ROS experiments clearly indicate the presence of hydrogen peroxide, however it is not known if hydroxyl radical formation is also involved. To test this, we have treated the cells with 100μM iron chelator Desferal, which would remove ferrous ions and inhibit the formation of hydroxyl radicals.

In our experiments Desferal caused a significant decrease of H2DCFDA signal levels (-29%; $p < 0,05$) and a significant increase in mitochondrial membrane potential (+21%; $p < 0,01$).

Desferal is an iron chelator which effectively removes the ferrous ion (Fe^{2+}) from the cytoplasm, preventing Fenton reaction which produces hydroxyl radicals, which in their turn, are also detectable by H2DCFDA probe. The fact that hydroxyl radicals are known to activate oxidative stress and damage to mitochondria may explain the the increase in Δψm after treatment with Desferal. Alternatively ferrous ions can independently of hydroxyl radicals induce lipid peroxidation in mitochondrial membrane and impair mitochondrial function [25]. The latter explanation is supported by the fact that mannitol, a scavenger of hydroxyl radical, did not have any effect.

hAMSC Conclusion

hAMSC were exposed to eight different treatments; three of them caused statistically significant effect on Δψm and cytoplasmic ROS.

Out of five antioxidants tested (SOD, Catalase, Mannitol, MitoTEMPO, Thiourea) only mitochondrial antioxidant MitoTEMPO changed cytoplasmic ROS levels. As suggested in the literature, SOD and Catalase are large molecules which do not enter the cells and the fact that they did not change cytoplasmic ROS levels suggests that extracellular ROS do not contribute to intracellular ROS pool.

Instead, NOX (tentatively, NOX-4 isoform) is a major contributor to the ROS in the cytoplasm in hAMSC; NOX can be inhibited by DPI. Also active mitochondrial respiration producing hydrogen peroxide contributes to the intracellular ROS levels. The following scheme (Fig. 36) demonstrates observed ROS-related metabolic pathways in hAMSC.
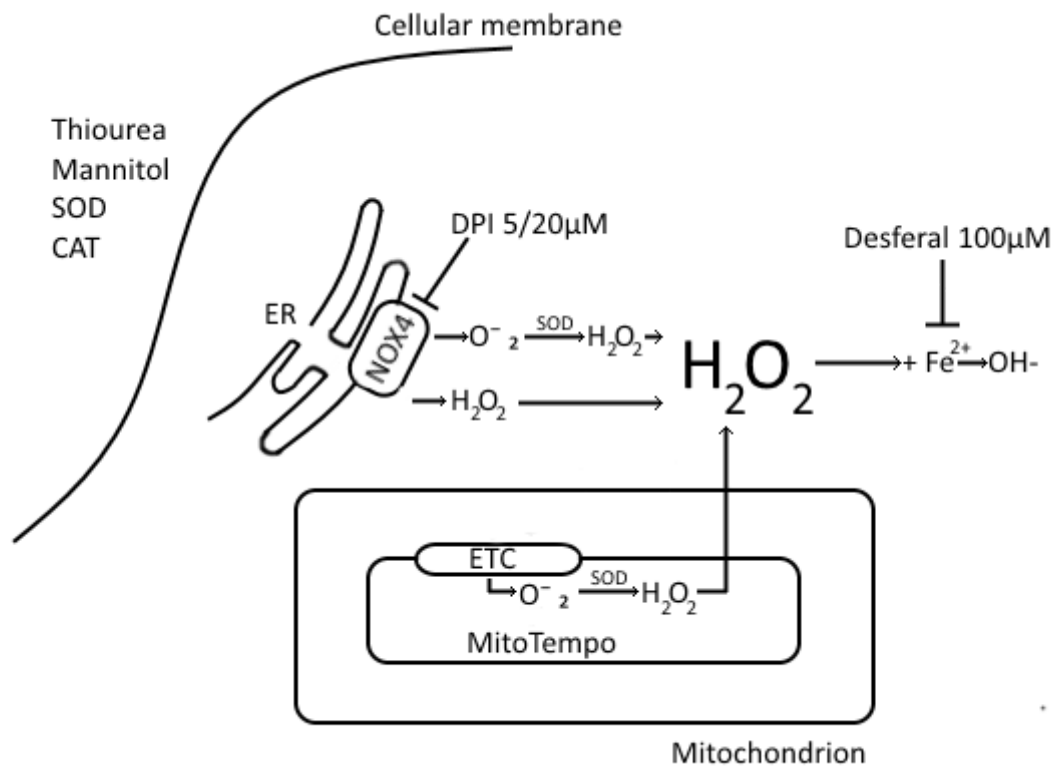
Fig 36. The main observed ROS metabolic pathways in hAMSC.

Metabolic pathways of ROS in MG-63

NOX in MG-63 osteoblast-like cells

Based on the results from hAMSC, DPI was selected as a compound of primary interest to investigate whether we could observe similar results in osteoblast-like cells.

In contrast, to hAMSC, osteoblast-like MG-63 cells did not respond to the treatment with 10µM DPI after 24 hours in terms of intracellular ROS levels, although a decrease in mitochondrial membrane potential was observed (-14%; $p < 0,01$).

The lack of effect on the cellular ROS levels by DPI can be explained by different NOX isoform expression. Literature research suggested that MG-63 primarily express NOX-2 isoform, which is located on the cellular membrane and produces ROS in the extracellular space. However, single publications also reported expression of NOX-4 in MG-63 cell line.

Objective. We assumed that cell line MG-63 is less sensitive to DPI than primary cells and increased the DPI concentration up to 100µM DPI in order to test whether higher DPI concentration can reduce cytoplasmic ROS levels in MG-63 cells, similarly to hAMSC.

However, after 24 hour incubation with 100µM DPI, osteoblast-like cells have lost the ability to adhere to the bottom of the slide by 24 hours, and no observable cells were found during examination under the microscope, suggesting that 100µM DPI had a toxic effect. To better understand the mechanism underlying this toxic effect the exposure time was reduced from 24h to 30 minutes. Surprisingly in contrast to hAMSC, in MG-63 cells the incubation with 100µM DPI resulted in a dramatic increase in cellular ROS levels (+189%; $p < 0,01$) and a decrease in mitochondrial membrane potential (-35%; $p < 0,01$).

This observations cannot be explained by NOX inhibition, however, the literature suggests that DPI, being a flavoprotein inhibitor in general, can exert its inhibitory action on other flavoprotein complexes, such as mitochondrial electron transport chain, at higher concentrations. Inhibition of ETC is known to dramatically increase the production of ROS. To gather more evidence towards this interpretation, we investigated the mitochondrial origin of ROS.

Mitochondrial ROS in MG-63

Since NOX-based explanation could not be used to explain the observed phenomenon, we investigated the possibility that high concentration of DPI caused a ROS burst of mitochondrial origin.

For that, we utilized MitoSOX probe specific to superoxide detection and observed a very significant signal increase in 100µM DPI treatment group compared to the controls (+45%, $p < 0,01$). However, we also observed nuclear staining caused by MitoSOX, therefore the use of H2DCFDA probe was preferable.

DPI owes its NOX inhibitory properties to being a flavoprotein inhibitor in general, which also includes cytochrome P450 reductase which is essential for electron transfer from NADPH to cytochrome P450 and proper function of the electron transfer chain [26]. Inhibition of the electron transfer chain has been strongly associated with an increase of ROS production. However, this effect was observed only on higher DPI concentration load.

Mitochondrial ROS in excessive amounts was reported to be capable to induce mitochondrial permeability transition pore opening, which leads to membrane depolarization, loss of $\Delta\psi m$ and superoxide leak in the cytoplasm.

Mitochondrial superoxide leak is also known to activate ROS- induced ROS release, a chain reaction which propagates ROS from mitochondrion to mitochondrion, repeating the destructive cycle [27]. We theorize that this mechanism is responsible for the phenomena, which was observed in osteoblast-like cells.

To gather more evidence to support this theory, we pre-treated MG-63 cells with 20µM MitoTEMPO mitochondria-targeted superoxide scavenger for 30 minutes before application of 100µM DPI and compared it to the negative (DMSO) and positive (100µM DPI) control. If the hypothesis holds true, then MitoTEMPO should reduce or even prevent the cellular ROS level increase caused by DPI.

The results have shown that application MitoTEMPO is capable prevent increase of cellular ROS levels (+4%, p = 0,54), and partially prevent mitochondrial membrane potential loss caused by high DPI concentrations (-15%; p > 0,01) compared to the negative control group.

This data further supports our assumption that superoxide production stimulated by high DPI levels is located in mitochondria [28].

Since H2DCFDA probe does not directly react which superoxide, the increase in DSF detectable ROS can be explained by the reaction of this fluorescent dye with secondary products of superoxide. DSF can react either with hydrogen peroxide or with peroxynitrite. The latter product is formed in the fast reaction between superoxide and nitric oxide, a signaling molecule ($NO + O_2^- = ONOO^-$).

Consequently, we examined if MG-63 cells can generate NO.

The presence of nitric oxide in MG-63 cell line was confirmed by utilizing NO-selective DAF-FM fluorescent probe (Fig. 3).

Based on this observation, we presume a possibility of peroxynitrite formation in osteoblast-like cells in response to higher dose DPI treatment due to innate presence of the nitric oxide. Thus, peroxynitrite formation in the cytoplasm is another factor most probably impairing MG-63 cells and possibly causing apoptosis.

MG-63 conclusion

The major finding of this study is that stem (hAMSC) and differentiated (MG-63) cell have different ROS metabolism. Unlike hAMSC, MG-63 cellular ROS levels did not change in response to lower concentrations of NOX inhibitor DPI (10µM). We hypothesize that this is due to different patterns of NOX isoform expression in both type of cells. We assume that MG-63 cell line primarily expresses NOX-2 which produces ROS in the extracellular space. Application of higher DPI concentration (100µM) causes a cascade of effects, which tentatively include the following steps. DPI impairs mitochondrial function elevating ROS generation, ROS activate permeability transition pore, the latter causes a drop in mitochondrial membrane potential and diffusion of mitochondrial ROS in cytoplasm. Here they activate death pathways (e.g. apoptosis) Interestingly, this demonstrates that DPI at lower concentration can act as an anti-oxidant agent (inhibiting NOX), but upon reaching a certain threshold DPI causes a pro-oxidative effect (via generation of mitochondrial ROS). This effect can be partially mitigated with MitoTEMPO mitochondrial antioxidant, which supports the theory of mitochondrial origin of ROS induced by 100µM DPI. The increase of H2DCFDA signal can additionally be explained by elevated activity of SOD or the formation of peroxynitrite. The following scheme (Fig. 37) demonstrates observed ROS-related metabolic pathways in MG-63.
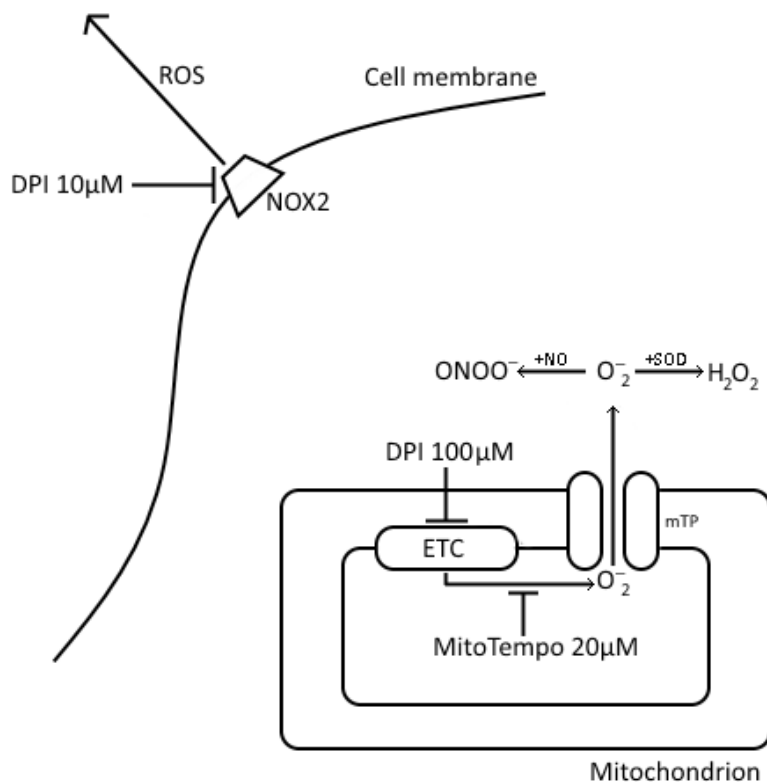
Fig 37. The main observed ROS metabolic pathways in MG-63.

Limitations

MG-63 osteoblast-like cell line are derived from osteosarcoma, and are considered to exhibit feature variety characteristic for undifferentiated osteoblast phenotype [29]. This has a direct implication that the majority of the cells in culture are arrested in pre-osteoblast state and the mineralisation is inconsistent, making this cell line an inferior candidate for tissue and grafting model applications. However, the response to hormonal treatments and integrin protein profile is similar to primary osteoblast culture, which is an indication that MG-63 cell line may serve as a suitable osteoblast model for metabolic process studies.

Sadly, due to COVID-19 situation development we did not accomplish the hAMSC treatment experiment with higher DPI concentrations to check whether the same mitochondria-related pro-oxidative effect can be observed. MG-63 cell line was also not treated with 1µM MitoTEMPO and concentrations for 24 hours to investigate if mitochondrial respiration also contributes to the cellular ROS levels via SOD catalysis of mitochondrial superoxide to hydrogen peroxide. In addition, 100µM Desferal treatment of osteoblast-like cells could shed the light if formation of hydroxyl radical is possible in this cell line. These experiments lie in a field of future perspectives.

CONCLUSION

To summarize, this thesis explored the differences in reactive oxygen species (ROS) metabolism in amniotic mesenchymal stem cells and one of their possible differentiation lineages to osteoblasts. A long time ROS were considered as deleterious species inducing oxidative stress. More recently ROS have been recognized as important signaling molecules, it is crucial to have a clear understanding of their origin and biological role. This knowledge provides insights regarding involved metabolic pathways and makes them an attractive target for further research due to ROS dualistic nature. For example, by carefully manipulating ROS levels it is possible to beneficially affect proliferation pathways or induce deleterious oxidative stress.

The proposed hypothesis is that upon differentiation to a specific lineage stem cells, the origin and action of ROS can be changed and these changes cause substantial differences in response of cells to compounds known to be capable on exerting effect on ROS.

By using laser scan microscopy and a variety of chemical treatments targeting specific pathways linked to the generation of ROS with particular emphasis on the impact of NOX and mitochondria, we analyzed the response of hAMSC and MG-63 osteoblast-like cell line, after 24 hours incubation with specific activators and inhibitors of ROS mediated pathways.

1. The results indicate that mitochondrial ROS production contributes to ROS presence in the cytoplasm and the formation of hydroxyl radical in cytoplasm is probable in hAMSC. Also, mesenchymal stem cells and osteoblast-like cells were exposed to NOX inhibitor DPI and different responses were observed, which suggests the differences in NOX isoforms. Our data suggest that in hAMSC NOX4 produces ROS in the cytoplasm. However, this pathway was not observed in osteoblast-like MG-63 cells. Our data suggest that MG-63 cells produce ROS in the extracellular space.

2. We observed that DPI, a commonly used NADPH-oxidase inhibitor can either reduce or enhance the levels of cytoplasmic ROS, depending on concentrations used. Further experiments were performed in order to understand the mechanisms underlying this phenomenon.

3. Our data suggest that the decay in cytoplasmic ROS levels at low concentrations of DPI is due to inhibition of NOX, while an increase in cytoplasmic ROS levels at higher DPI concentration is due to the elevated release ROS from mitochondria. We observed that at high concentrations. DPI induced superoxide burst of mitochondrial origin in osteoblast-like cells. This leads to the leak of ROS from mitochondria, tentatively via mitochondrial membrane transition pore opening accompanied by mitochondrial membrane potential decrease, and it also most probably promotes formation of toxic peroxynitrite within the cells. This damage can be partially mitigated by anti-oxidant MitoTEMPO. The phenomena of superoxide induction by DPI may be utilized to create a testing ground for antioxidant compounds.

4. This study has, however, two important limitations apply, as:

(i) MG-63 osteoblast-like cell line is not a primary osteoblast culture. Nevertheless, most associated limitations apply to inconsistent mineralisation and respective grafting issues, which is unrelated to the research topic.

(ii) Higher concentration DPI-induced ROS burst and respective mechanisms were only tested on MG-63 cells due to COVID-19 situation development. We are going to address these issues in the future.

REFERENCES

[1] Zimorski V, Ku C, Martin WF. Endosymbiotic theory for organelle origins. Gould SB Curr Opin Microbiol. 2014; doi:10.1016/j.mib.2014.09.008

[2] Hu L, Yin C, Zhao F, Ali A, Ma J, Qian A. Mesenchymal Stem Cells: Cell Fate Decision to Osteoblast or Adipocyte and Application in Osteoporosis Treatment. Int J Mol Sci. 2018;19(2):360. doi:10.3390/ijms19020360

[3] Czekanska E, Stoddart M, Richards R, Hayes J. In search of an osteoblast cell model for in vitro research. Eur. Cells Mater. 2012;24:1–17. doi: 10.22203/eCM.v024a01.

[4] Buck T, Hack CT, Berg D, et al. The NADPH oxidase 4 is a major source of hydrogen peroxide in human granulosa-lutein and granulosa tumor cells. Sci Rep 9, 3585. 2019. doi:10.1038/s41598-019-40329-8

[5] Wegener G, Volke V. Nitric Oxide Synthase Inhibitors as Antidepressants. Pharmaceuticals (Basel). 2010;3(1):273-299. doi:10.3390/ph3010273

[6] Zhi -Wu Yu, Quinn PJ. Dimethyl sulphoxide: A review of its applications in cell biology. Biosci Rep 1 December 1994; 14 (6): 259–281. doi:10.1007/BF01199051

[7] Pal R, Mamidi MK, Das AK, et al. Diverse effects of dimethyl sulfoxide (DMSO) on the differentiation potential of human embryonic stem cells. Arch Toxicol 86, 651–661.2012. doi:10.1007/s00204-011-0782-2

[8] Zorova LD, Popkov VA, Plotnikov EY, et al. Mitochondrial membrane potential. Anal Biochem. 2018;552:50–59. doi:10.1016/j.ab.2017.07.009

[9] Ameziane El Hassani R, Dupuy C. Detection of Intracellular Reactive Oxygen Species (CM-H2DCFDA), 2013 . BIO-PROTOCOL. 3. doi:10.21769/BioProtoc.313

[10] Thermofischer Scientific Molecular Probes, Nitric oxide indicators: DAF-FM and DAF-FM Diacetate. Catalog number D23844, Product Information, accessed 03.06.2020.

[11] Thermofischer Scientific Molecular Probes, MitoSOX™ Red mitochondrial superoxide indicator for live-cell imaging. Catalog number M36008, Product information, accessed 03.06.2020

[12] Murphy MP. How mitochondria produce reactive oxygen species. Biochem J. 2009;417(1):1–13. doi:10.1042/BJ20081386

[13] Reynolds MR, Singh I, Azad TD, et al. Heparan sulfate proteoglycans mediate Aβ-induced oxidative stress and hypercontractility in cultured vascular smooth muscle cells. Mol Neurodegeneration 11, 9.2016. doi:10.1186/s13024-016-0073-8

[14] Vejražka M, Míček R, Štípek S. Apocynin inhibits NADPH oxidase in phagocytes but stimulates ROS production in non-phagocytic cells. Biochim. Biophys. Acta Gen. Subj., 1722 (2005), pp. 143-147. doi:10.1016/j.bbagen.2004.12.008

[15] Quan M, Cai CL, Valencia GB, Aranda JV, Beharry KD. MnTBAP or Catalase Is More Protective against Oxidative Stress in Human Retinal Endothelial Cells Exposed to Intermittent Hypoxia than Their Co-Administration (EUK-134). React Oxyg Species (Apex). 2017;3(7):47-65. doi:10.20455/ros.2017.801

[16] Belda JI, Artola A, Garcıa-Manzanares, MD, et al. Hyaluronic acid combined with mannitol to improve protection against freeradical endothelial damage: experimental model. J. Cataract Refract. Surg. 31, 1213–1218. 2005. doi:10.1016/j.jcrs.2004.11.055

[17] National Center for Biotechnology Information. PubChem Compound Summary for CID 6251, Mannitol. https://pubchem.ncbi.nlm.nih.gov/compound/Mannitol. Accessed 03.05.2020.

[18] Pandey M, Srivastava AK, D'Souza SF, Penna S. Thiourea, a ROS scavenger, regulates source-to-sink relationship to enhance crop yield and oil content in Brassica juncea (L.). PLoS One. 2013;8(9):e73921. doi:10.1371/journal.pone.0073921

[19] Laurindo FR, Araujo TL, Abrahão TB. Nox NADPH oxidases and the endoplasmic reticulum. Antioxid Redox Signal. 2014;20(17):2755-2775. doi:10.1089/ars.2013.5605

[20] Albensi BC. Dysfunction of mitochondria: Implications for Alzheimer's disease. Int Rev Neurobiol. 2019;145:13-27. doi:10.1016/bs.irn.2019.03.001

[21] Tarabová B , Lukeš P , Hammer MU , et al. Fluorescence measurements of peroxynitrite/peroxynitrous acid in cold air plasma treated aqueous solutions. Chem Phys. 2019;21(17):8883-8896. doi:10.1039/c9cp00871c

[22] Zalba G, San Jose G, Moreno MU, Fortuno MA, Fortuno A, Beaumont FJ, Diez J. Oxidative stress in arterial hypertension: role of NAD(P)H oxidase. Hypertension 2001;38:1395-9. doi:10.1161/hy1201.099611

[23] Dikalov S. Cross talk between mitochondria and NADPH oxidases. Free Radic Biol Med. 2011;51(7):1289-1301. doi:10.1016/j.freeradbiomed.2011.06.033

[24] Biochimica et Biophysica Acta (BBA) – Biomembranes. Volume 1758, Issue 8, August 2006, Pages 994-1003. doi:10.1016/j.bbamem.2006.183433

[25] Dungel P, Perlinger M, Weidinger A, Redl H, Kozlov AV. The cytoprotective effect of nitrite is based on the formation of dinitrosyl iron complexes. Free Radic Biol Med. 2015;89:300-310. doi:10.1016/j.freeradbiomed.2015.08.012

[26] McGuire JJ, Anderson DJ, McDonald BJ, Narayanasami R, Bennett BM. Inhibition of NADPH-cytochrome P450 reductase and glyceryl trinitrate biotransformation by diphenyleneiodonium sulfate. Biochem Pharmacol. 1998;56(7):881-893. doi:10.1016/s0006-2952(98)00216-0

[27] Zorov DB, Juhaszova M, Sollott SJ. Mitochondrial reactive oxygen species (ROS) and ROS-induced ROS release. Physiol Rev. 2014;94(3):909-950. doi:10.1152/physrev.00026.2013

[28] Lambert A, Buckingham J, Boysen H, Brand M. Diphenyleneiodonium acutely inhibits reactive oxygen species production by mitochondrial complex I during reverse, but not forward electron transport. Biochimica et biophysica acta. 1777. 397-403. doi:10.1016/j.bbabio.2008.03.005.

[29] Clover J, Gowen M. Are MG-63 and HOS TE85 human osteosarcoma cell lines representative models of the osteoblastic phenotype?. Bone. 1994;15(6):585-591. doi:10.1016/8756-3282(94)90305-0